Supporting Information

High-Performance Allosteric Conditional Guide RNAs for Mammalian Cell-Selective Regulation of CRISPR/Cas

Lisa M. Hochrein[†], Heyun Li[‡], and Niles A. Pierce[†,§,*]

Contents

[†]Division of Biology & Biological Engineering, California Institute of Technology, Pasadena, CA 91125, USA. [‡]Division of Chemistry & Chemical Engineering, California Institute of Technology, Pasadena, CA 91125, USA. [§]Division of Engineering & Applied Science, California Institute of Technology, Pasadena, CA 91125, USA. *Email: niles@caltech.edu

List of Figures

List of Tables

S1 Methods

S1.1 Step-by-step summary of cgRNA design and validation in mammalian cells.

Step 1: Select cgRNA logic and Cas function

- Select: ON → OFF cgRNA logic
- Select: inducing dCas9 (dCas9-VPR)
- Implement logic: "if not X then Y"

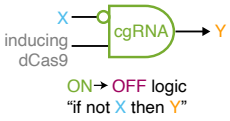

Step 2: Select cgRNA mechanism

- Select allosteric terminator switch mechanism (Figure 4a)
- X and Y sequences are fully independent

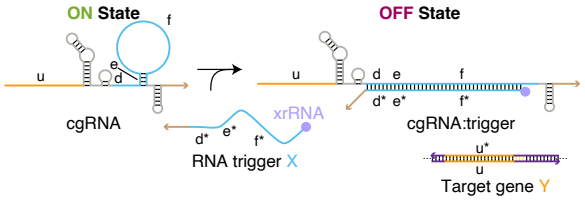

Step 3: Formulate and perform computational sequence design (Section S1.2)

- Select target gene Y (fluorescent reporter Phi-YFP)
- Design N orthogonal systems (e.g., N=4)
- Set domain dimensions
  - ldl = 6 nt, lel = 4 nt, lfl = 30 nt
- Formulate target test tubes
  - Reactants tube for each system (Q, R, S, T)
  - Products tube for each system (Q, R, S, T)
  - One global crosstalk tube
  - Total of 4 reactant tubes + 4 product tubes + 1 global crosstalk tube = 9 target test tubes
- Specify sequence constraints
- Specify defect weights
- Perform sequence design using NUPACK
- Add xrRNA protective element to 5′ end of triggers

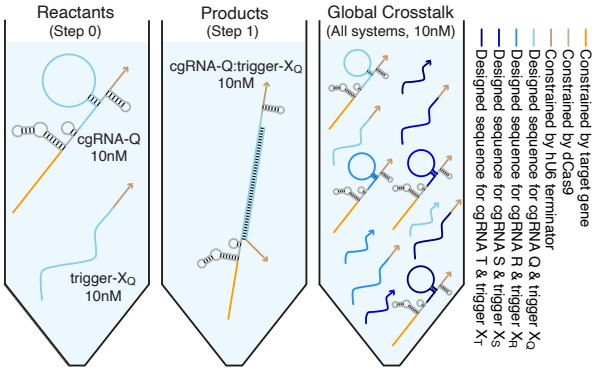

cgRNA Q

5′–GAGTCGCGTGTAGCGAAGCAGTTTTAGAGCTAGAAATAGCAAGTTAAAATAAGGCTAGTCCGATCTTTGCGCGTTAGTTTCGTTCGTATTTCTGTCATGTTTGCGCGGCACCGAGTCGGTGCTTTTTTT–3′

Trigger X_Q

5′–AGTCAGGCCACTTGTGCCACGGTTTGAGCAAACCGTGCTGCCTGTAGCTCCGCCAATAATGGGAGGCGTAAACATGACAGAAATACGAACGAAACTAACGCGCAAAGATCTTTTTTT–3′

Step 4: Construct materials and perform experiments (Section S1.3)

- For each system, construct cgRNA plasmid and trigger plasmid with fluorescent protein (FP) transfection control for each plasmid
- Construct dCas9-VPR plasmid and Phi-YFP plasmid to serve as target gene Y
- Culture cells (HEK 293T cells)
- Transfect 4 plasmids (Lipofectamine 2000)
- Perform flow cytometry experiments
- Gate data for single cells that highly express FP transfection controls for cgRNA and trigger plasmids

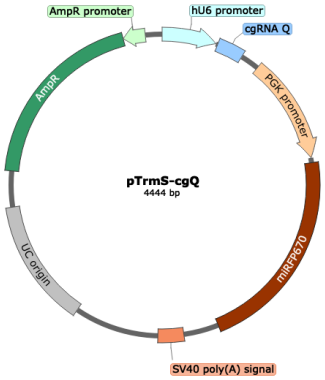

Step 5: Analyze data (Section S1.4)

- Plot histograms of single-cell fluorescence intensities (Figures 4c, S15, S16)
- Plot raw data summary (Figure 4d)
- Plot derived quantities
  - Fold change (Figure 4e)
  - Fractional dynamic range (Figure 4f)
  - Crosstalk (Figure 4g)

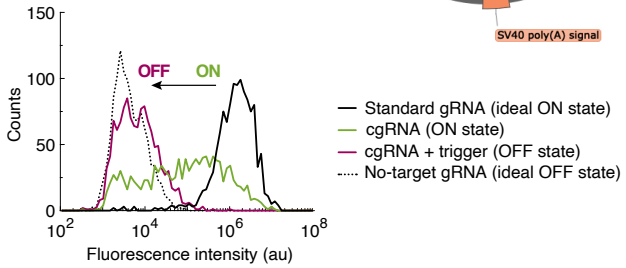

Figure S1: Step-by-step summary of cgRNA design and validation in mammalian cells.

S1.2 Rational design of libraries of orthogonal cgRNAs using NUPACK

For each mechanism, orthogonal cgRNA/trigger pairs were designed using the reaction pathway engineering tools within NUPACK (`nupack.org`; see the NUPACK 3.2 User Guide).[3,4] Sequence design was formulated as a multistate optimization problem using target test tubes to represent reactant and product states of cgRNA/trigger hybridization, as well as to model crosstalk between orthogonal cgRNAs (Figure 6).[4] Each target test tube contains a set of desired on-target complexes, each with a target secondary structure and target concentration, and a set of undesired off-target complexes, each with vanishing target concentration. Target test tubes were specified using the general formulation of Section S2.2.1 in the Supplementary Information of Wolfe et al.[4] using the definitions provided below (Section S1.2.1 for the terminator switch and Section S1.2.2 for the split-terminator switch).

Sequence designs were performed for libraries of 4 orthogonal cgRNA/trigger pairs for the terminator switch and 10 orthogonal cgRNA/trigger pairs for the split-terminator switch. For a given design trial, the sequences were optimized by mutating the sequence set to reduce the multi-tube ensemble defect quantifying the average fraction of incorrectly paired nucleotides over the multi-tube ensemble.[4–6] Optimization of the ensemble defect implements both a positive design paradigm, explicitly designing for on-pathway elementary steps, and a negative-design paradigm, explicitly designing against off-pathway crosstalk.[4] Sequence design was performed subject to diverse sequence constraints as detailed below (complementarity constraints inherent to the reaction pathway [d complementary to d*, etc], as well as biological sequence constraints imposed by the trigger X, the regulatory target Y, the protein effector (dCas9), or the hU6 terminator). Within the ensemble defect, defect weights (see Section S1.6 in the Supplementary Information of Wolfe et al.[4]) were applied to prioritize design effort as described below. Designs were performed using RNA parameters for 37 °C in 1M Na^+.[7]

After performing several independent design trials for a given mechanism, a final sequence set was selected for experimental testing based on inspection of the predicted structural defects (fraction of nucleotides in the incorrect base-pairing state within the ensemble of an on-target complex) and concentration defects (fraction of nucleotides in the incorrect base-pairing state because there is a deficiency in the concentration of an on-target complex) for species in the context of the target test tubes,[4,6] as well as for each cgRNA in the presence of each non-cognate trigger. After completing sequence design, the xrRNA version of each trigger was made by appending the Dengue 4 xrRNA motif[1] to the 5′ end. For the ON→OFF terminator switch mechanism, after preliminary experimental screening, 4 out of 4 cgRNA/trigger pairs (Q, R, S, T) were selected for full experimental characterization (of these, we previously studied Q, R, and S without the 5′ xrRNA on the triggers[8]). For the OFF→ON split-terminator switch mechanism, sequence design was initially performed for exploratory studies with sequence domain "d" of length 40 nt, which we tested experimentally along with truncated versions with $|\mathrm{d}| = \{30, 20, 10\}$ nt (Figure S27). We decided to focus on the 10 nt dimension, designing a set of 10 orthogonal cgRNA/trigger pairs, from which we selected 3 designs (M, N, O) for further experimental study. We also tested truncated versions of those three designs with $|\mathrm{d}| = \{8, 6, 4\}$ nt (Figure S29). We performed a full experimental characterization of the M, N, O designs with $|\mathrm{d}|$ = 10 nt (Figure S28) and $|\mathrm{d}|$ = 4 nt (Figure 5).

S1.2.1 Target test tube specification for ON→OFF terminator switch mechanism

To design N orthogonal systems, the total number of target test tubes is $|\Omega| = \sum_{n=1,\ldots,N} \{\text{Step 0, Step 1}\}_n$ + Crosstalk = $2N + 1$; the target test tubes in the multi-tube ensemble, Ω, are indexed by $h = 1, \ldots, |\Omega|$. $L_{\max} = 2$ for all tubes (i.e., each target test tube contains all off-target complexes of up to 2 strands). Final sequence designs for orthogonal cgRNAs (Q, R, S, T) and triggers (X_Q, X_R, X_S, X_T) are shown in Table S5.

Reactants for system *n*

- cgRNAs: G_n
- Triggers: X_n

Elementary step tubes for system *n*

- Step 0_n tube: $\Psi_{0_n}^{\text{products}} \equiv \{G, X\}_n$; $\Psi_{0_n}^{\text{reactants}} \equiv \emptyset$; $\Psi_{0_n}^{\text{exclude}} \equiv \{G{\cdot}X\}_n$ (downstream on-pathway product)
- Step 1_n tube: $\Psi_{1_n}^{\text{products}} \equiv \{G{\cdot}X\}_n$; $\Psi_{1_n}^{\text{reactants}} \equiv \{G, X\}_n$; $\Psi_{1_n}^{\text{exclude}} \equiv \emptyset$

Global crosstalk tube

- Crosstalk tube: $\Psi_{\text{global}}^{\text{reactive}} \equiv \cup_{n=1,\ldots,N}\{\lambda_n^{\text{reactive}}\}$; $\Psi_{\text{global}}^{\text{crosstalk}} \equiv \Psi_{\text{global}}^{L\leq L_{\max}} - \cup_{n=1,\ldots,N}\{\lambda_n^{\text{cognate}}\}$

The reactive species and cognate products for system n are:

- $\lambda_n^{\text{simple}} \equiv \{G, X\}_n$
- $\lambda_n^{\text{ss-out}} \equiv X_n$
- $\lambda_n^{\text{ss-in}} \equiv G_n^{\text{ss}}$ (30 nt single stranded terminator loop insert domain)
- $\lambda_n^{\text{reactive}} \equiv \{G, X, G^{\text{ss}}\}_n$
- $\lambda_n^{\text{cognate}} \equiv \{G{\cdot}X, G^{\text{ss}}{\cdot}X\}_n$

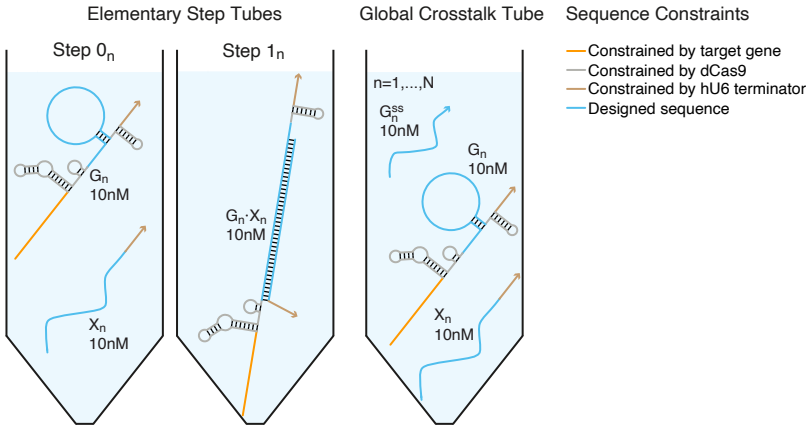

Tube	On-targets (Ψ_h^{on})	Off-targets (Ψ_h^{off})
Step 0_n	$\{G, X\}_n$	$\Psi_{0_n}^{L\leq L_{\max}} - \{G{\cdot}X\}_n$
Step 1_n	$\{G{\cdot}X\}_n$	$\{G, X\}_n \cup \Psi_{1_n}^{L\leq L_{\max}}$
Crosstalk	$\cup_{n=1,\ldots,N}\{\lambda_n^{\text{reactive}}\}$	$\Psi_{\text{global}}^{L\leq L_{\max}} - \cup_{n=1,\ldots,N}\{\lambda_n^{\text{cognate}}\}$

Figure S2: Target test tubes for sequence design of orthogonal terminator switch cgRNAs. Top: Target test tube schematics. Bottom: Target test tube details. Each target test tube contains the depicted on-target complexes (each with the depicted target structure and a target concentration of 10 nM) and the off-target complexes listed in the table (each with vanishing target concentration). The on-target structures depicted above are used in the mechanism schematic of Figure 4a. To simultaneously design N orthogonal systems, the total number of target test tubes is $|\Omega| = 2N + 1$. $L_{\max} = 2$ for all tubes. Domain shading reflects sequence constraints. Design conditions: RNA in 1 M Na^+ at 37 °C.

Domain dimensions

- |d| = 6 nt
- |e| = 4 nt
- |f| = 30 nt

Sequence constraints

- Assignment constraints: portions of the cgRNA are constrained to match standard gRNA sequences for use with dCas9 (shaded gray in Figure 4a, Figure S2, and Tables S5), the hU6 terminator is fully constrained (shaded tan in Figure 4a, Figure S2, and Table S5).
- Watson–Crick constraints: cgRNA sequence domains "d-e-f" are constrained to be complementary to the trigger sequence domains "f*-e*-d*" (shaded blue in Figure 4a, Figure S2, and Tables S5).
- Assignment constraint: cgRNA domain "u" is constrained to be complementary to the binding region located in front of the minimal CMV promoter in the reporter plasmid P1-minCMV-PhiYFP (constrained sequence shaded orange in Figure 4a, Figure S2, and Tables S5).
- Pattern prevention constraints: the following patterns are prevented for cgRNA sequence domains "d", "e", and "f": `AAAA`, `CCCC`, `GGGG`, `UUUU`, `KKKKKK`, `MMMMMM`, `RRRRRR`, `SSSSSS`, `WWWWWW`, `YYYYYY`.

Defect weights

- Test tube weight for each elementary step tube: 1
- Test tube weight for global crosstalk tube: 4
- Nucleotide weights are depicted for each complex in Figure S3

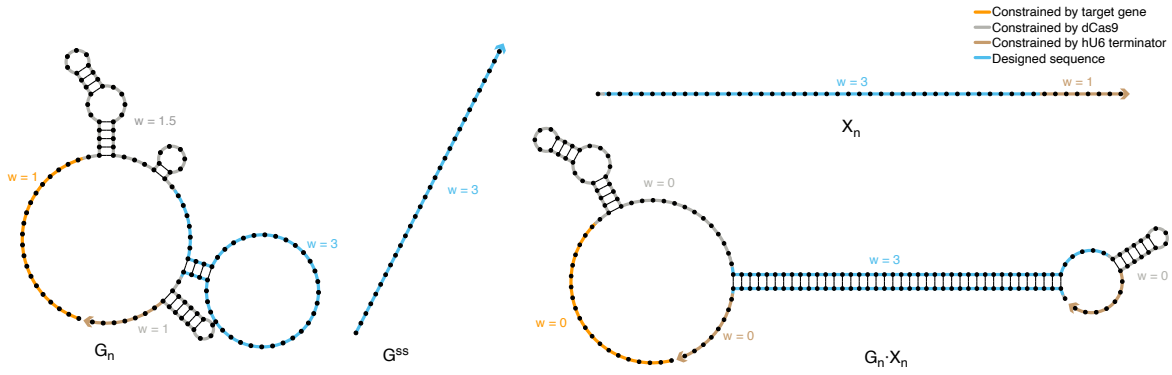

Figure S3: Nucleotide defect weights for sequence design of terminator switch cgRNAs. Within the target test tubes of Figure S2, the nucleotides in a given sequence domain within a given complex are assigned a defect weight *w* as depicted.

S1.2.2 Target test tube specification for OFF→ON split-terminator switch mechanism

To design N orthogonal systems, the total number of target test tubes is $|\Omega| = \sum_{n=1,\ldots,N} \{\text{Step 0, Step 1}\}_n$ + Crosstalk = $2N + 1$; the target test tubes in the multi-tube ensemble, Ω, are indexed by $h = 1, \ldots, |\Omega|$. $L_{\max} = 2$ for all tubes (i.e., each target test tube contains all off-target complexes of up to 2 strands). Final sequence designs for orthogonal cgRNAs (M, N, O) and triggers (X_M, X_N, X_O) are shown in Table S6 for designs with domain "d" of length 10 nt as well as for truncated versions with domain "d" truncated to be 8, 6, or 4 nt.

Reactants for system *n*

- cgRNA fragment 1: G_n
- cgRNA fragment 2: X_n

Elementary step tubes for system *n*

- Step 0_n tube: $\Psi_{0_n}^{\text{products}} \equiv \{G, X\}_n$; $\Psi_{0_n}^{\text{reactants}} \equiv \{\emptyset\}_n$; $\Psi_{0_n}^{\text{exclude}} \equiv \{G{\cdot}X\}_n$ (downstream on-pathway product)
- Step 1_n tube: $\Psi_{1_n}^{\text{products}} \equiv \{G{\cdot}X\}_n$; $\Psi_{1_n}^{\text{reactants}} \equiv \{G, X\}_n$; $\Psi_{1_n}^{\text{exclude}} \equiv \emptyset$

Global crosstalk tube

- Crosstalk tube: $\Psi_{\text{global}}^{\text{reactive}} \equiv \cup_{n=1,\ldots,N}\{\lambda_n^{\text{reactive}}\}$; $\Psi_{\text{global}}^{\text{crosstalk}} \equiv \Psi_{\text{global}}^{L \le L_{\max}} - \cup_{n=1,\ldots,N}\{\lambda_n^{\text{cognate}}\}$

The reactive species and cognate products for system n are:

- $\lambda_n^{\text{simple}} \equiv \{G, X\}_n$
- $\lambda_n^{\text{ss-out}} \equiv \{G^d\}_n$ (10 nt domain "d" that forms terminator duplex)
- $\lambda_n^{\text{ss-in}} \equiv \{X^{d^*}\}_n$ (10 nt domain "d*" that forms terminator duplex)
- $\lambda_n^{\text{reactive}} \equiv \{G^d, X^{d^*}\}_n$
- $\lambda_n^{\text{cognate}} \equiv \{G^d{\cdot}X^{d^*}\}_n$

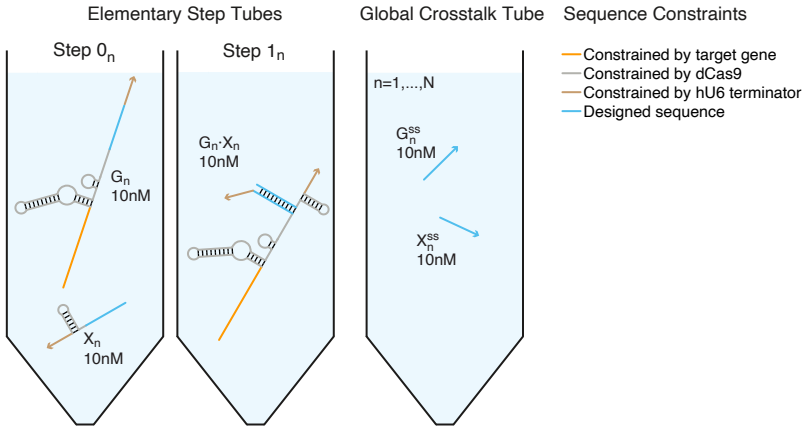

Tube	On-targets (Ψ_h^{on})	Off-targets (Ψ_h^{off})
Step 0_n	$\{G, X\}_n$	$\Psi_{0_n}^{L \le L_{\max}} - \{G{\cdot}X\}_n$
beginalign3pt] Step 1_n	$\{G{\cdot}X\}_n$	$\{G, X\}_n \cup \Psi_{1_n}^{L \le L_{\max}}$
beginalign3pt] Crosstalk	$\cup_{n=1,\ldots,N}\{\lambda_n^{\text{reactive}}\}$	$\Psi_{\text{global}}^{L \le L_{\max}} - \cup_{n=1,\ldots,N}\{\lambda_n^{\text{cognate}}\}$

Figure S4: Target test tubes for sequence design of orthogonal split-terminator switch cgRNAs. Top: Target test tube schematics. Bottom: Target test tube details. Each target test tube contains the depicted on-target complexes (each with the depicted target structure and a target concentration of 10 nM) and the off-target complexes listed in the table (each with vanishing target concentration). The on-target structures depicted above are used in the mechanism schematic of Figure 5a. To simultaneously design N orthogonal systems, the total number of target test tubes is $|\Omega| = 2N + 1$. $L_{\max} = 2$ for all tubes. Domain shading reflects sequence constraints. Design conditions: RNA in 1 M Na^+ at 37 °C.

Domain dimensions

- |d| = 10 nt

Sequence constraints

- Assignment constraints: portions of the cgRNA are constrained to match standard gRNA sequences (with the FE modified Cas9 handle[9]) for use with dCas9 (shaded gray in Figure 5a, Figure S4, and Table S6), the hU6 terminator is fully constrained (shaded tan in Figure 5a, Figure S4, and Table S6).
- Watson–Crick constraints: sequence domain "d" is constrained to be complementary to the sequence domains "d*" (shaded blue in Figure 5a, Figure S4, and Table S6).
- Assignment constraint: cgRNA domain "u" is constrained to be complementary to the binding region located in front of the minimal CMV promoter in the reporter plasmid P1-minCMV-PhiYFP (constrained sequence shaded orange in Figure 5a, Figure S4, and Tables S6).
- Pattern prevention constraints: the following patterns are prevented for cgRNA sequence domain "d": `AAAA`, `CCCC`, `GGGG`, `UUUU`, `KKKKKK`, `MMMMMM`, `RRRRRR`, `SSSSSS`, `WWWWWW`, `YYYYYY`.

Defect weights

- Test tube weight for each elementary step tube: 1
- Test tube weight for global crosstalk tube: 20 (for design of 10 orthogonal systems)
- Nucleotide weights are depicted for each complex in Figure S5

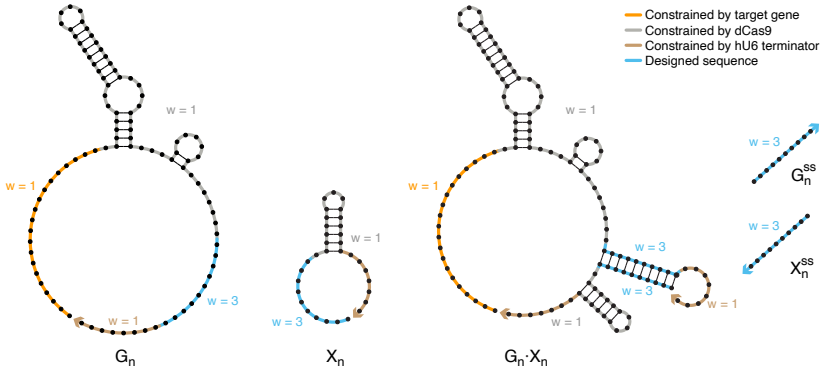

Figure S5: Nucleotide defect weights for sequence design of the split-terminator switch cgRNAs. Within the target test tubes of Figure S4, the nucleotides in a given sequence domain within a given complex are assigned a defect weight *w* as depicted.

S1.3 Methods for cgRNA studies in HEK 293T cells

S1.3.1 Plasmid construction and molecular cloning

Sequences for parts used are provided in Section S2. Plasmid layouts for each construct as well as representative plasmid maps and corresponding full plasmid sequences are provided in Section S3.

gRNA, cgRNA and trigger constructs were generated via Golden Gate assembly. For cgRNA-expressing plasmids, the pU6_gRNA_handle_U6t plasmid (gift from T. Lu, Addgene plasmid #49016)[10] was mutated to remove the BsaI site in the ampicillin resistance gene, EBFP2 was replaced with miRFP670 cloned from the pmiRFP670-N1 plasmid (gift from V. Verkhusha, Addgene plasmid #79987),[11] and the gRNA scaffold was replaced with two BsaI sites and two BbsI sites for subsequent Golden Gate assembly. For trigger-expressing plasmids, the pU6_gRNA_handle_U6t plasmid was mutated to remove the BsaI site in the ampicillin resistance gene, and the gRNA scaffold was replaced with either two BsaI or two BpiI (BbsI) sites for subsequent Golden Gate assembly.

To generate the cgRNA and trigger plasmids, gene fragments containing both the cgRNA and trigger with the appropriate restriction recognition sites and overhangs were ordered from Twist Bioscience or fragments were generated by ligating RxnReady duplexes (Integrated DNA Technologies, IDT) to form the appropriate inserts (see Section S1.3.1 of Hanewich-Hollatz, *et al.* for additional details).[8] The fragment was then cloned into the appropriately modified pU6_gRNA_handle_U6t plasmid using the standard Golden Gate assembly guidelines provided by NEB (https://www.neb.com/protocols/2018/06/05/golden-gate-24-fragment-assembly-protocol). Plasmids were transformed into 5-α competent *E. coli* (NEB, #C2987) and clonally selected with carbenicillin (Teknova, #C2130). Plasmids were purified (Qiagen, #27104) and Sanger sequenced to verify the introduced sequences.

To create the random pool control plasmids, inverse PCR was used to replace the trigger sequence with an equivalent number of random nucleotides. To achieve this, primers were designed according to standard molecular cloning techniques to flank the trigger region and ordered from Integrated DNA Technologies (IDT). To incorporate random nucleotides, the appropriate number of N (machine mixed) nucleotides were added to the 5′ end of one of the primers. The PCR reactions used Q5 Hot Start High-Fidelity polymerase (NEB, #M0494) and were run according to the manufacturer's instructions. KLD enzyme mix (NEB, #M0554S) was used to ligate the PCR product and remove the template plasmid. Transformed 5-α competent *E. coli* (NEB, #C2987) were directly grown in liquid LB with carbenicillin (no clonal selection) and the plasmid pool was purified (Qiagen, #27104). Sanger sequencing showed all four nucleotides represented in the randomized region.

S1.3.2 Cell culture and induction assay

Mammalian cgRNA performance was assayed using a modified version of previously described fluorescent protein gene induction assays.[12–14] Briefly, four plasmids (Figure S6 and Table S1) were co-transfected into HEK 293T cells and CRISPR/dCas9-mediated fluorescent protein gene induction was assayed by flow cytometry after 24 h.

The SP-dCas9-VPR plasmid was a gift from G. Church (Addgene plasmid #63798).[15] The reporter plasmid P1-minCMV-PhiYFP was synthesized and cloned by Twist Bioscience. The insert sequence was based on the reporter-gT1 plasmid (Addgene plasmid #47320)[12] and was modified to replace the T1 gRNA target-binding region with a P1 gRNA target-binding region[13] and the dTomato fluorescent protein was replaced with the PhiYFP fluorescent protein from P1-EYFP-pA (Addgene plasmid #55197).[13]

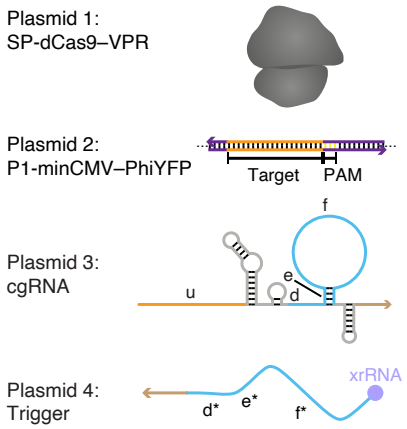

Figure S6: Assay schematic.

Plasmid	Function	Fluorescent protein	Parent plasmid
SP-dCas9-VPR	*S. pyogenes* dCas9 fused to VPR induction domains (CMV promoter)	none	Addgene #63798
P1-minCMV-PhiYFP	P1 gRNA binding site upstream of a minimal CMV promoter expressing PhiYFP reporter	PhiYFP	Twist Amp High Copy, Addgene #47320 & #55197
cgRNA	hU6 expression of a single cgRNA	miRFP670 (pPGK)	Addgene #49016
Trigger	hU6 expression of a single trigger	EBFP2 (pPGK)	Addgene #49016

Table S1: HEK 293T induction assay components.

HEK 293T (ATCC, #CRL-3216) cells were cultured in high-glucose DMEM (Gibco, #11995073) supplemented with 10% FBS (Gibco, #16140071) and grown at 37 °C with 5% CO_2. Cells were subcultivated every 2 to 3 days at a ratio of 1:5 to 1:10 for a maximum of two months. Plasmids (Table S13) were transiently transfected using Lipofectamine 2000 (Thermo Fisher Scientific, #11668019) according to manufacturer's instructions. One day prior to transfection, 24-well plates were seeded with 125,000 cells in 0.5 mL medium per well. For each well, a total of 500 ng plasmid was transfected simultaneously (Table S2) with 2.5 μL Lipofectamine 2000. For cgRNA-only studies, the equivalent amount of plasmids from a random trigger pool were used in place of the trigger plasmid. 24 hours post transfection, the cells were detached from the plate with 100 μL Accumax (#AM105) at RT for 5 min. 200 μL flow cytometry buffer [2.5 mg/mL fraction V BSA (VWR, #0332), 10 mM pH 7.5 HEPES buffer (Teknova, #H1035), 50 μg/mL DNase1 (Sigma-Aldrich, #D4513), 1 mM $MgCl_2$ (Ambion, #AM9530G) in 1X HBSS (Gibco, #14175)] was added to each well and the entire solution was triturated. 200 μL/well of cell solution was filtered through a 96-well 30–40 μM PP/PE non-woven media filter plate (Pall, AcroPrep Advance Filter Plate, #8027) into a round bottom 96-well plate.

	Terminator switch		**Split-terminator switch**	
Plasmid	ng/well transfected	Relative copy number	ng/well transfected	Relative copy number
SP-dCas9-VPR	19.1	0.15	19.1	0.03
P1-minCMV-PhiYFP	60.5	1.29	60.5	0.29
cgRNA	50.0	1.00	216.6	1.00
trigger	370.4	7.90	203.8	1.00
Figures	3, 4, S16, S17, S20, S21, S22, S23, S24		5, S18, S19, S26, S27, S28, S29, S30	

Table S2: Amount of plasmid transfected per well of a 24-well plate.

S1.3.3 Flow cytometry

Protein fluorescence was measured with the CytoFLEX S Flow Cytometer (Beckman Coulter) in the Caltech Flow Cytometry Facility. SSC-H vs. FSC-H was used to gate for live cells, followed by FSC-H vs. FSC-W to gate for single cells (see example in Figure S7). 100,000 live cells (or a maximum of 180 μL sample) were collected for each well at a flow rate of 60 μL/min. EBFP2 fluorescence (trigger plasmid transfection control) was measured using the 405 nm laser with the 450/45 nm filter. miRFP670 fluorescence (cgRNA plasmid transfection control) was measured using the 640 nm laser with the 660/20 nm filter. PhiYFP fluorescence (target gene Y) was measured using the 488 nm laser with the 525/40 nm filter. Using the standard gRNA, high PhiYFP expression resulted in saturation of the detector for some cells (see histograms of Figure S7b).

Flow cytometry fluorescence values were compensated using control samples expressing a single fluorescent protein and the built-in compensation calculation tools. The compensation required was minimal due to good spectral separation between the fluorescent proteins. Live, single cells were then gated to include only cells with high levels of both fluorescent protein transfection controls calculated by first determining the cut-off signal for the top 5% of cells in each channel (area) for each well and then calculating the median of the cut-off values across wells for each channel. The same threshold values were applied to all wells from the same experiment; the thresholds were allowed to vary between experiments based on the transfection control signal from a given experiment.

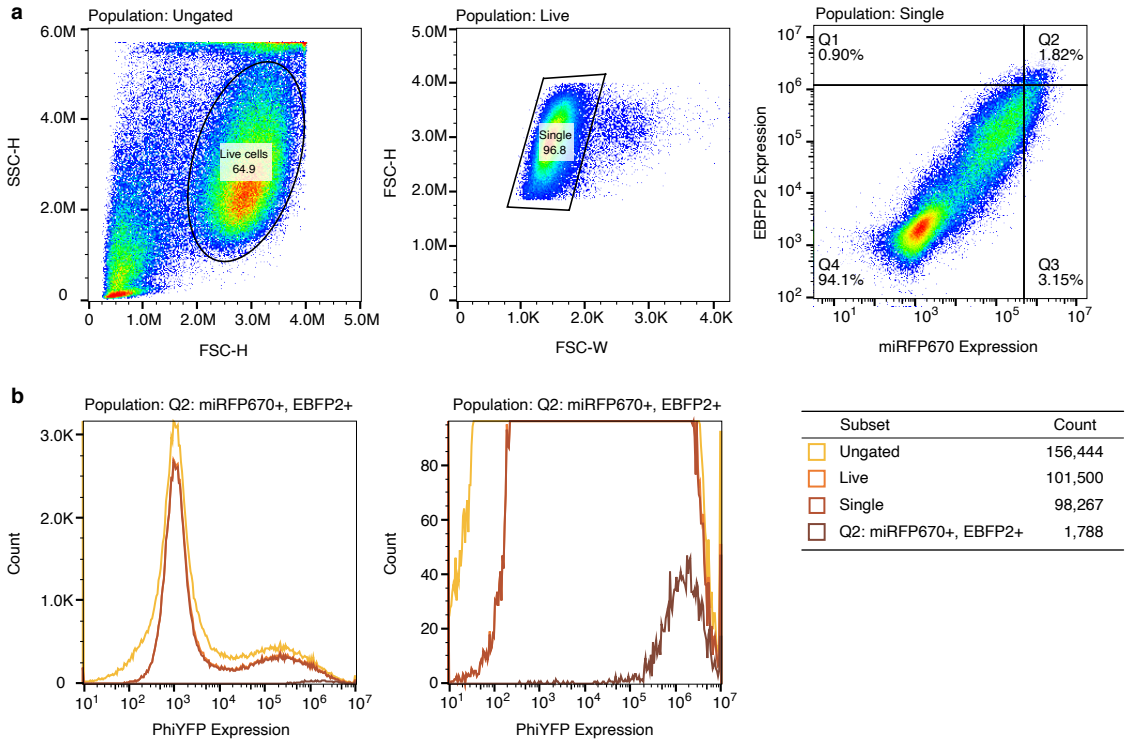

Figure S7: Illustration of the gates used for flow cytometry analysis of HEK 293T cells. (a) Example of progressive gating for one replicate of the standard gRNA with the random trigger pool. First, live cells are gated using side scatter height (SSC-H) vs. forward scatter height (FSC-H). Live cells are then gated for single cells using forward scatter height (FSC-H) vs. forward scatter width (FSC-W). Finally, only highly transfected cells are included in the analysis (Q2: miRFP670+ and EBFP2+). (b) PhiYFP fluorescence intensity histogram for ungated sample, live-cell gated sample, single-cell gated sample, and [miRFP670+ and EBFP2+] gated sample. Left: full y axis. Right: zoom on y axis.

Upon gating for high-expressing cells, cell counts varied (Table S3).* Bar graphs (e.g., Figures 3, 4, 5) display fluorescence measurements based on all cells in the highly-transfected gate. Flow cytometry replicates are shown in Section S5. To facilitate comparisons, fluorescence distributions display $M = 1200$ cells ($M = 1000$ cells for Figures 3c and S23) for all experiment types and replicates for a given cgRNA; distributions display the last-measured cells from the highly transfected gate (after first removing any cells with non-positive fluorescence readings to enable display in a log plot).

cgRNA mechanism	EBFP2 threshold (AU)	miRFP670 threshold (AU)	Cells gated	Figures
xrRNA variants	1,520,730	884,996	487–3906	3b, S21, S22
Terminator switch: xrRNA comparison	1,451,700	1,015,410	1067–4358	3c, S23, S24
Terminator switch	1,148,140	534,136	1545–3970	4, S16, S17
Terminator switch: FE modification	1,396,870	450,349	1240–4516	S20
Standard gRNA truncation	359,975	1,003,265	2114–3085	S26
Split-terminator switch: truncation experiments, from $\|d\| = 10$ nt	424,918	864,536	1864–4155	S29
Split-terminator switch: $\|d\| = 4$ nt	608,615	865,180	1017–2394	5, S18, S19
Split-terminator switch: $\|d\| = 10$ nt	746,518	2,408,290	1244–2313	S28
Split-terminator switch: xrRNA comparison $\|d\| = 4$ nt	562,801	1,228,150	1537–5081	S30

Table S3: Transfection control threshold values and cell counts.

*See Section S6.6 for alternative gating approached using for the exploratory study of Figure S27.

S1.4 Quantitative fluorescence analysis for HEK 293T cells

S1.4.1 Measuring reporter assay signal in HEK 293T cells

For HEK 293T cells utilizing the CRIPSR/Cas9 gene induction assay, the total fluorescence (SIG + BACK) in the relevant fluorescent channel (PhiYFP) is a combination of signal (SIG) from cgRNA-mediated induction of PhiYFP gene expression and background (BACK) consisting of the autofluorescence inherent to the cells plus basal expression of PhiYFP from the minimal CMV promoter. Let (n, p) denote wells transfected with cgRNA n and trigger p. Background fluorescence is characterized using a no-target gRNA lacking the target-binding region ($n =$ 'no-target'). For cell j of replicate well i using cgRNA n and trigger p, we denote the background:

$$X(\text{no-target}, p)_{i,j}^{\text{BACK}}, \tag{S1}$$

the signal:

$$X(n, p)_{i,j}^{\text{SIG}}, \tag{S2}$$

and the total fluorescence (SIG + BACK):

$$X(n, p)_{i,j}^{\text{SIG+BACK}}. \tag{S3}$$

For replicate well i, we measure the mean fluorescence ($\bar{X}(n, p)_i^{\text{SIG+BACK}}$ for cells expressing cgRNA n, $\bar{X}(\text{no-target}, p)_i^{\text{BACK}}$ for cells expressing a 'no-target' control) over all the cells in the [miRFP670+ and EBFP2+] gate (corresponding to cells highly expressing cgRNA and trigger plasmid transfection controls). Performance across $N = 3$ replicate wells is characterized by the sample means ($\bar{X}(n, p)^{\text{SIG+BACK}}$ and $\bar{X}(\text{no-target}, p)^{\text{BACK}}$) and estimated standard errors of the mean ($s_{\bar{X}(n,p)^{\text{SIG+BACK}}}$ and $s_{\bar{X}(\text{no-target},p)^{\text{BACK}}}$). The mean signal is estimated as[†]

$$\bar{X}(n, p)^{\text{SIG}} = \bar{X}(n, p)^{\text{SIG+BACK}} - \bar{X}(\text{no-target}, p)^{\text{BACK}} \tag{S4}$$

with the standard error of the mean estimated via uncertainty propagation as

$$s_{\bar{X}(n,p)^{\text{SIG}}} \leq \sqrt{(s_{\bar{X}(n,p)^{\text{SIG+BACK}}})^2 + (s_{\bar{X}(\text{no-target},p)^{\text{BACK}}})^2}. \tag{S5}$$

The upper bound on estimated standard error of the mean holds under the assumption that the correlation between SIG and BACK is non-negative.

S1.4.2 Fold change for constitutively active cgRNAs (ON→OFF logic) with inducing dCas9

For a constitutively active cgRNA with inducing dCas9 (terminator switch of Figure 4), the ON state for cgRNA n corresponds to high fluorescence using no trigger ($p = 0$; no-trigger control using a random pool of triggers to provide a sequence-generic approximation of the metabolic load of trigger expression) and the OFF state corresponds to low fluorescence using cognate trigger ($p = n$). The ON state is estimated as

$$\bar{X}(n)^{\text{ON}} = \bar{X}(n, 0)^{\text{SIG}}, \tag{S6}$$

the OFF state is estimated as

$$\bar{X}(n)^{\text{OFF}} = \bar{X}(n, n)^{\text{SIG}}, \tag{S7}$$

and the fold change is estimated as

$$\bar{X}(n)^{\text{ON:OFF}} = \bar{X}(n, 0)^{\text{SIG}} / \bar{X}(n, n)^{\text{SIG}} \tag{S8}$$

with standard error of the mean estimated via uncertainty propagation as

$$s_{\bar{X}(n)^{\text{ON:OFF}}} \leq \bar{X}(n)^{\text{ON:OFF}} \sqrt{\left(\frac{s_{\bar{X}(n,0)^{\text{SIG}}}}{\bar{X}(n, 0)^{\text{SIG}}}\right)^2 + \left(\frac{s_{\bar{X}(n,n)^{\text{SIG}}}}{\bar{X}(n, n)^{\text{SIG}}}\right)^2}. \tag{S9}$$

The upper bound on estimated standard error of the mean holds under the assumption that the correlation between SIG in the two transfection conditions is non-negative. The ON state, OFF state, and fold change are tabulated in Table S14.

[†]For some supporting studies (Figures S24 and S30) we estimate the background independent of the specific trigger, p, using a no-trigger control ($p = 0$) that employs a random pool of triggers to provide a sequence-generic approximation of the metabolic load of trigger expression. The mean background is then denoted $\bar{X}(\text{no-target}, 0)^{\text{BACK}}$ with standard error of the mean $s_{\bar{X}(\text{no-target},0)}$.

S1.4.3 Fold change for constitutively inactive cgRNAs (OFF→ON logic) with inducing dCas9

For a constitutively inactive cgRNA with inducing dCas9 (split-terminator switch of Figure 5), the ON state for cgRNA n corresponds to high fluorescence using cognate trigger ($p = n$) and the OFF state corresponds to low fluorescence using no trigger ($p = 0$; no-trigger control using a random pool of triggers to provide a sequence-generic approximation of the metabolic load of trigger expression). The ON state is estimated as

$$\bar{X}(n)^{\mathrm{ON}} = \bar{X}(n,n)^{\mathrm{SIG}}, \tag{S10}$$

the OFF state is estimated as

$$\bar{X}(n)^{\mathrm{OFF}} = \bar{X}(n,0)^{\mathrm{SIG}}, \tag{S11}$$

and the fold change is estimated as

$$\bar{X}(n)^{\mathrm{ON:OFF}} = \bar{X}(n,n)^{\mathrm{SIG}} / \bar{X}(n,0)^{\mathrm{SIG}} \tag{S12}$$

with standard error of the mean estimated via uncertainty propagation as

$$s_{\bar{X}(n)^{\mathrm{ON:OFF}}} \leq \bar{X}(n)^{\mathrm{ON:OFF}} \sqrt{\left(\frac{s_{\bar{X}(n,n)^{\mathrm{SIG}}}}{\bar{X}(n,n)^{\mathrm{SIG}}}\right)^2 + \left(\frac{s_{\bar{X}(n,0)^{\mathrm{SIG}}}}{\bar{X}(n,0)^{\mathrm{SIG}}}\right)^2}. \tag{S13}$$

The upper bound on estimated standard error holds under the assumption that the correlation between SIG in the two transfection conditions is non-negative. The ON state, OFF state, and fold change are tabulated in Table S14.

S1.4.4 Dynamic range for constitutively active cgRNAs (ON→OFF logic) with inducing dCas9

For a constitutively active cgRNA with inducing dCas9 (terminator switch of Figure 4), the ON state for cgRNA n corresponds to high fluorescence using no trigger ($p = 0$; no-trigger control using a random pool of triggers to provide a sequence-generic approximation of the metabolic load of trigger expression) and the OFF state corresponds to low fluorescence using cognate trigger ($p = n$). The dynamic range is estimated as

$$\bar{X}(n)^{\mathrm{DR}} = \bar{X}(n,0)^{\mathrm{SIG}} - \bar{X}(n,n)^{\mathrm{SIG}} \tag{S14}$$

with standard error of the mean estimated via uncertainty propagation as

$$s_{\bar{X}(n)^{\mathrm{DR}}} \leq \sqrt{(s_{\bar{X}(n,0)^{\mathrm{SIG}}})^2 + (s_{\bar{X}(n,n)^{\mathrm{SIG}}})^2}. \tag{S15}$$

The upper bound on estimated standard error of the mean holds under the assumption that the correlation between SIG in the two transfection conditions is non-negative. Dynamic range is tabulated in Table S14.

S1.4.5 Dynamic range for constitutively inactive cgRNAs (OFF→ON logic) with inducing dCas9

For a constitutively inactive cgRNA with inducing dCas9 (split-terminator switch of Figure 5), the ON state for cgRNA n corresponds to high fluorescence using cognate trigger ($p = n$) and the OFF state corresponds to low fluorescence using no trigger ($p = 0$; no-trigger control using a random pool of triggers to provide a sequence-generic approximation of the metabolic load of trigger expression). The dynamic range is estimated as

$$\bar{X}(n)^{\mathrm{DR}} = \bar{X}(n,n)^{\mathrm{SIG}} - \bar{X}(n,0)^{\mathrm{SIG}} \tag{S16}$$

with standard error of the mean estimated via uncertainty propagation as

$$s_{\bar{X}(n)^{\mathrm{DR}}} \leq \sqrt{(s_{\bar{X}(n,n)^{\mathrm{SIG}}})^2 + (s_{\bar{X}(n,0)^{\mathrm{SIG}}})^2}. \tag{S17}$$

The upper bound on estimated standard error of the mean holds under the assumption that the correlation between SIG in the two transfection conditions is non-negative. Dynamic range is tabulated in Table S14.

S1.4.6 Fractional dynamic range for cgRNAs with inducing dCas9

For a cgRNA with inducing dCas9 (terminator switch of Figure 4 and split-terminator switch of Figure 5), the ideal OFF state corresponds to low fluorescence with a no-target gRNA lacking the target-binding region ($n =$ 'no-target') and the ideal ON state corresponds to high fluorescence with a standard gRNA ($n =$ 'standard') with a target-binding region for the target Y. Both the no-target gRNA control and the standard gRNA control incorporate a no-trigger control ($p = 0$) using a random pool of triggers to provide a sequence-generic approximation of the metabolic load of trigger expression. The ideal dynamic range is estimated as

$$\bar{X}^{\mathrm{DR}}_{\mathrm{ideal}} = \bar{X}(\text{standard}, 0)^{\mathrm{SIG}} - \bar{X}(\text{no-target}, 0)^{\mathrm{SIG}} \tag{S18}$$

with standard error of the mean estimated via uncertainty propagation as

$$s_{\bar{X}^{\mathrm{DR}}_{\mathrm{ideal}}} \leq \sqrt{(s_{\bar{X}(\text{standard},0)^{\mathrm{SIG}}})^2 + (s_{\bar{X}(\text{no-target},0)^{\mathrm{SIG}}})^2}. \tag{S19}$$

The upper bound on estimated standard error of the mean holds under the assumption that the correlation between SIG in the two transfection conditions is non-negative. The fractional dynamic range is estimated as

$$\bar{X}(n)^{\mathrm{FDR}} = \bar{X}(n)^{\mathrm{DR}} / \bar{X}^{\mathrm{DR}}_{\mathrm{ideal}} \tag{S20}$$

with standard error of the mean estimated via uncertainty propagation as

$$s_{\bar{X}(n)^{\mathrm{FDR}}} \leq \bar{X}(n)^{\mathrm{FDR}} \sqrt{\left(\frac{s_{\bar{X}(n)^{\mathrm{DR}}}}{\bar{X}(n)^{\mathrm{DR}}}\right)^2 + \left(\frac{s_{\bar{X}^{\mathrm{DR}}_{\mathrm{ideal}}}}{\bar{X}^{\mathrm{DR}}_{\mathrm{ideal}}}\right)^2}. \tag{S21}$$

The upper bound on estimated standard error of the mean holds under the assumption that the correlation between the ideal dynamic range and the cgRNA dynamic range is non-negative. Fractional dynamic range is tabulated in Table S14.

S1.4.7 Crosstalk for orthogonal cgRNAs

Crosstalk (CT) is estimated for cgRNA n with trigger p as

$$\bar{X}(n,p)^{\mathrm{CT}} = [\bar{X}(n,p)^{\mathrm{SIG}} - \bar{X}(n,0)^{\mathrm{SIG}}] / [\bar{X}(n,n)^{\mathrm{SIG}} - \bar{X}(n,0)^{\mathrm{SIG}}] \tag{S22}$$

with the standard error of the mean estimated via uncertainty propagation as

$$s(n,p)^{\mathrm{CT}} \leq \left|\bar{X}(n,p)^{\mathrm{CT}}\right| \sqrt{\left(\frac{\sqrt{(s_{\bar{X}(n,p)^{\mathrm{SIG}}})^2 + (s_{\bar{X}(n,0)^{\mathrm{SIG}}})^2}}{\bar{X}(n,p)^{\mathrm{SIG}} - \bar{X}(n,0)^{\mathrm{SIG}}}\right)^2 + \left(\frac{\sqrt{(s_{\bar{X}(n,n)^{\mathrm{SIG}}})^2 + (s_{\bar{X}(n,0)^{\mathrm{SIG}}})^2}}{\bar{X}(n,n)^{\mathrm{SIG}} - \bar{X}(n,0)^{\mathrm{SIG}}}\right)^2}. \tag{S23}$$

The upper bound on estimated standard error holds under the assumption that the correlation between transfection conditions is non-negative. Note that crosstalk values can be positive or negative. The crosstalk modulus is $\left|\bar{X}(n,p)^{\mathrm{CT}}\right|$. Crosstalk is tabulated in Table S15.

S2 Sequences for cgRNAs, triggers, and controls

	Name	Sequence	Figure	Legend
a	**Standard gRNA with standard or FE modified Cas9 handle**			
	P1-g	5′–GAGTCGCGTGTAGCGAAGCAGTTTTAGAGCTAGAAATAGCAAGTTAAAATAAGGCTAGTCCGTTATCAACTTGAAAAAGTGGCACCGAGTCGGTGCTTTTTTT–3′	3c, 4cd, S16, S17, S22ab, S23, S24a, S26	Standard gRNA
	P1-g-FE	5′–GAGTCGCGTGTAGCGAAGCAGTTTAAGAGCTATGCTGGAAACAGCATAGCAAGTTTAAATAAGGCTAGTCCGTTATCAACTTGAAAAAGTGGCACCGAGTCGGTGCTTTTTTT–3′	5cd, S18, S19, S20cd, S28cd, S30ab	Standard gRNA
b	**No-target gRNA with standard or FE modified Cas9 handle**			
	NT-g	5′–GTTTTAGAGCTAGAAATAGCAAGTTAAAATAAGGCTAGTCCGTTATCAACTTGAAAAAGTGGCACCGAGTCGGTGCTTTTTTT–3′	3c, 4cd, S16, S17, S22b, S23, S24a, S26	No-target gRNA
	NT-g-FE	5′–GTTTAAGAGCTATGCTGGAAACAGCATAGCAAGTTTAAATAAGGCTAGTCCGTTATCAACTTGAAAAAGTGGCACCGAGTCGGTGCTTTTTTT–3′	5cd, S18, S19, S20cd, S28cd, S30ab	No-target gRNA
c	**No-trigger random pool with or without xrRNA**			
	TrmS-40	5′–NNNNNNNNNNNNNNNNNNNNNNNNNNNNNNNNNNNNNNNNCTTTTTTT–3′	3c(left), S23(left)	All except: cgRNA + trigger
			S22b	No-trigger
			S24a	− Trigger (−xrRNA)
	TrmS-xr-40	5′–AGTCAGGCCACTTGTGCCACGGTTTGAGCAAACCGTGCTGCCTGTAGCTCCGCCAATAATGGGAGGCGTNNNNNNNNNNNNNNNNNNNNNNNNNNNNNNNNNNNNNNCTTTTTTT–3′	3b, S21,	No trigger
			3c(right), 4c, S16	All except: cgRNA + trigger
			S17, S20c, S23(right)	
			S22ab	xr11-no-trigger
			S24a	− Trigger (+xrRNA)
			S27, 4d, S20d	− Trigger
			S26	All samples
	STS-xr-25	5′–AGTCAGGCCACTTGTGCCACGGTTTGAGCAAACCGTGCTGCCTGTAGCTCCGCCAATAATGGGAGGCGTNNNNNNNNNNNNNNNNNNNNNNNNNNCTTTTTT–3′	S28c	All except: cgRNA + trigger
			S28d, S29b	− Trigger
	STS-19	5′–NNNNNNNNNNNNNNNNNNNCTTTTTTT–3′	5c, S18, S19, S30a(left)	All except: cgRNA + trigger
			5d	− Trigger
			S30b	− Trigger (−xrRNA)
	STS-xr-19	5′–AGTCAGGCCACTTGTGCCACGGTTTGAGCAAACCGTGCTGCCTGTAGCTCCGCCAATAATGGGAGGCGTNNNNNNNNNNNNNNNNNNNCTTTTTTT–3′	S30a(right)	All except: cgRNA + trigger
			S30b	− Trigger (+xrRNA)

Table S4: Control gRNA and trigger sequences. (a) Standard gRNA with standard or FE modified Cas9 handle. (b) No-target gRNA with standard or FE modified Cas9 handle. No-target gRNAs lack a target-binding region. (c) No-trigger random pool with or without xrRNA. Nucleotides shaded orange are constrained by the target plasmid (P1 gRNA target-binding site). Nucleotides shaded gray are constrained by dCas9. The C nucleotide shaded black is a cloning artifact. Nucleotides shaded tan are constrained by the hU6 terminator sequence.[16] Nucleotides shaded lavender are constrained by the xrRNA sequence derived from the Dengue virus type 4 (Dengue 4, NC_002640.1).[1] N nucleotides (shaded red) denote a mixture of A, C, G, T.

	Name	Sequence	Figure	Legend
a	**Terminator switch cgRNAs with standard Cas9 handle**			
	TrmS-cgQ	5′-GAGTCGCGTGTAGCGAAGCAGTTTTAGAGCTAGAAATAGCAAGTTAAAAT AAGGCTAGTCCGATCTTTGCGCGTTAGTTTCGTTCGTATTTCTGTCATGTTT GCGCGGCACCGAGTCGGTGCTTTTTTT-3′	3bc, 4c, S16 4d, S17, S21, S22ab, S23, S24a	cgRNA cgRNA Q
	TrmS-cgR	5′-GAGTCGCGTGTAGCGAAGCAGTTTTAGAGCTAGAAATAGCAAGTTAAAAT AAGGCTAGTCCGTATCGCCGGGTTCAAGCAGATGTGGCATTTCAGTGTAGTT CCCGGGCACCGAGTCGGTGCTTTTTTT-3′	4d, S17, S23, S24a	cgRNA R
	TrmS-cgS	5′-GAGTCGCGTGTAGCGAAGCAGTTTTAGAGCTAGAAATAGCAAGTTAAAAT AAGGCTAGTCCGTCCATTCGGGTTTACTATTACAATCTTACGTGTTCTCATT CCCGGGCACCGAGTCGGTGCTTTTTTT-3′	4d, S17, S23, S24a	cgRNA S
	TrmS-cgT	5′-GAGTCGCGTGTAGCGAAGCAGTTTTAGAGCTAGAAATAGCAAGTTAAAAT AAGGCTAGTCCGGATAAAGGGAAAGATGAAGTGATGTGAAGATAGAGTTGGA TCCCGGCACCGAGTCGGTGCTTTTTTT-3′	4d, S17, S23, S24a	cgRNA T
b	**Terminator switch cgRNAs with FE modified Cas9 handle**			
	TrmS-cgQ-FE	5′-GAGTCGCGTGTAGCGAAGCAGTTTAAGAGCTATGCTGGAAACAGCATAG CAAGTTTAAATAAGGCTAGTCCGATCTTTGCGCGTTAGTTTCGTTCGTATT TCTGTCATGTTTGCGCGGCACCGAGTCGGTGCTTTTTTT-3′	S20c S20d	cgRNA cgRNA Q
	TrmS-cgR-FE	5′-GAGTCGCGTGTAGCGAAGCAGTTTAAGAGCTATGCTGGAAACAGCATAG CAAGTTTAAATAAGGCTAGTCCGTATCGCCGGGTTCAAGCAGATGTGGCAT TTCAGTGTAGTTCCCGGGCACCGAGTCGGTGCTTTTTTT-3′	S20d	cgRNA R
	TrmS-cgS-FE	5′-GAGTCGCGTGTAGCGAAGCAGTTTAAGAGCTATGCTGGAAACAGCATAG CAAGTTTAAATAAGGCTAGTCCGTCCATTCGGGTTTACTATTACAATCTTA CGTGTTCTCATTCCCGGGCACCGAGTCGGTGCTTTTTTT-3′	S20d	cgRNA S
	TrmS-cgT-FE	5′-GAGTCGCGTGTAGCGAAGCAGTTTAAGAGCTATGCTGGAAACAGCATAG CAAGTTTAAATAAGGCTAGTCCGGATAAAGGGAAAGATGAAGTGATGTGAA GATAGAGTTGGATCCCGGCACCGAGTCGGTGCTTTTTTT-3′	S20d	cgRNA T
c	**Terminator switch triggers**			
	TrmS-tQ	5′-AAACATGACAGAAATACGAACGAAACTAACGCGCAAAGATCTTTTTTT-3′	3bc(left), S21 S22b S23(left) S24a	Trigger X_Q Trigger X_Q Trigger X_Q (−xrRNA)
	TrmS-tR	5′-AACTACACTGAAATGCCACATCTGCTTGAACCCGGCGATACTTTTTTT-3′	S23(left) S24a	Trigger X_R Trigger X_R (−xrRNA)
	TrmS-tS	5′-AATGAGAACACGTAAGATTGTAATAGTAAACCCGAATGGACTTTTTTT-3′	S23(left) S24a	Trigger X_S Trigger X_S (−xrRNA)
	TrmS-tT	5′-TCCAACTCTATCTTCACATCACTTCATCTTTCCCTTTATCCTTTTTTT-3′	S23(left) S24a	Trigger X_T Trigger X_T (−xrRNA)
d	**Terminator switch triggers with xrRNA**			
	TrmS-xr-tQ	5′-AGTCAGGCCACTTGTGCCACGGTTTGAGCAAACCGTGCTGCCTGTAGCTC CGCCAATAATGGGAGGCGTAAACATGACAGAAATACGAACGAAACTAACGCG CAAAGATCTTTTTTT-3′	3b 3c(right), 4c, S16, S20c 4d, S17, S20d, S23(right) S21 S22b S24a	Dengue Trigger Trigger X_Q xr11 xr11-X_Q Trigger X_Q (+xrRNA)
	TrmS-xr-tR	5′-AGTCAGGCCACTTGTGCCACGGTTTGAGCAAACCGTGCTGCCTGTAGCTC CGCCAATAATGGGAGGCGTAACTACACTGAAATGCCACATCTGCTTGAACCC GGCGATACTTTTTTT-3′	4d, S17, S20d, S23(right) S24a	Trigger X_R Trigger X_R (+xrRNA)
	TrmS-xr-tS	5′-AGTCAGGCCACTTGTGCCACGGTTTGAGCAAACCGTGCTGCCTGTAGCTC CGCCAATAATGGGAGGCGTAATGAGAACACGTAAGATTGTAATAGTAAACCC GAATGGACTTTTTTT-3′	4d, S17, S20d, S23(right) S24a	Trigger X_S Trigger X_S (+xrRNA)
	TrmS-xr-tT	5′-AGTCAGGCCACTTGTGCCACGGTTTGAGCAAACCGTGCTGCCTGTAGCTC CGCCAATAATGGGAGGCGTTCCAACTCTATCTTCACATCACTTCATCTTTCC CTTTATCCTTTTTTT-3′	4d, S17, S20d, S23(right) S24a	Trigger X_T Trigger X_T (+xrRNA)

Table S5: Terminator switch sequences (ON→OFF logic). (a) Terminator switch cgRNAs with standard Cas9 handle. (b) Terminator switch cgRNAs with FE modified Cas9 handle. (c) Terminator switch triggers. (d) Terminator switch triggers with xrRNA. Nucleotides shaded orange are constrained by the target binding site on the reporter plasmid. Nucleotides shaded gray are constrained by dCas9. Nucleotides shaded blue are designed as described in Section S1.2. The C nucleotide shaded black is a cloning artifact. Nucleotides shaded tan are constrained by the hU6 terminator sequence.[16] Nucleotides shaded lavender are constrained by the xrRNA sequence (xr11) derived from the Dengue virus type 4 (Dengue 4, NC_002640.1).[1]

	Name	Sequence	Figure	Legend
a	**Split-terminator switch cgRNAs with FE modified Cas9 handle**			
	STS-cgM	5′–GAGTCGCGTGTAGCGAAGCAGTTTAAGAGCTATGCTGGAAACAGCATAGC	5c, S18, S30a	cgRNA
		AAGTTTAAATAAGGCTAGTCCGTTATCAGCACCTTTTTTT–3′	5d, S19, S30b	cgRNA M
			S29b	4nt cgRNA M
	STS-cgN	5′–GAGTCGCGTGTAGCGAAGCAGTTTAAGAGCTATGCTGGAAACAGCATAGC	5d, S19, S30b	cgRNA N
		AAGTTTAAATAAGGCTAGTCCGTTATCAGGCCCTTTTTTT–3′	S29b	4nt cgRNA N
	STS-cgO	5′–GAGTCGCGTGTAGCGAAGCAGTTTAAGAGCTATGCTGGAAACAGCATAGC	5d, S19, S30b	cgRNA O
		AAGTTTAAATAAGGCTAGTCCGTTATCACCCACTTTTTTT–3′	S29b	4nt cgRNA O
b	**Split-terminator switch triggers**			
	STS-tM	5′–GTGCGGCACCGAGTCGGTGCTTTTTTT–3′	5c, S18, S30a(left)	Trigger
			5d, S19	Trigger X_M
			S30b	Trigger X_M (−xrRNA)
	STS-tN	5′–GGCCGGCACCGAGTCGGTGCTTTTTTT–3′	5d, S19	Trigger X_N
			S30b	Trigger X_N (−xrRNA)
	STS-tO	5′–TGGGGGCACCGAGTCGGTGCTTTTTTT–3′	5d, S19	Trigger X_O
			S30b	Trigger X_O (−xrRNA)
c	**Split-terminator switch triggers with xrRNA**			
	STS-xr-tM	5′–AGTCAGGCCACTTGTGCCACGGTTTGAGCAAACCGTGCTGCCTGTAGCTC	S29b	4nt Trigger X_M
		CGCCAATAATGGGAGGCGTGTGCGGCACCGAGTCGGTGCTTTTTTT–3′	S30a(right)	Trigger
			S30b	Trigger X_M (+xrRNA)
	STS-xr-tN	5′–AGTCAGGCCACTTGTGCCACGGTTTGAGCAAACCGTGCTGCCTGTAGCTC	S29b	4nt Trigger X_N
		CGCCAATAATGGGAGGCGTGGCCGGCACCGAGTCGGTGCTTTTTTT–3′	S30b	Trigger X_N (+xrRNA)
	STS-xr-tO	5′–AGTCAGGCCACTTGTGCCACGGTTTGAGCAAACCGTGCTGCCTGTAGCTC	S29b	4nt Trigger X_O
		CGCCAATAATGGGAGGCGTTGGGGGCACCGAGTCGGTGCTTTTTTT–3′	S30b	Trigger X_O (+xrRNA)

Table S6: Split-terminator switch sequences (OFF→ON logic). (a) Split-terminator switch cgRNAs with FE modified Cas9 handle. (b) Split-terminator switch triggers. (c) Split-terminator switch triggers with xrRNA. Nucleotides shaded orange are constrained by the target binding site on the reporter plasmid. Nucleotides shaded gray are constrained by dCas9. Nucleotides shaded blue are designed as described in Section S1.2. The C nucleotide shaded black is a cloning artifact. Nucleotides shaded tan are constrained by the hU6 terminator sequence.[16] Nucleotides shaded lavender are constrained by the xrRNA sequence (xr11) derived from the Dengue virus type 4 (Dengue 4, NC_002640.1).[1]

	Name	Sequence	Figure	Legend
a	**MVE xrRNAs**			
	TrmS-MVE_xrRNA1_truncate-tQ	5′-TAGTCAGGCCAGCCGGTTAGGCTGCCACCGAAGGTTGGTAGACGGTGCT GCCTGCGACCAACAAACATGACAGAAATACGAACGAAACTAACGCGCAAAG ATCTTTTTTT-3′	S21	xr1
	TrmS-MVE_xrRNA1-tQ	5′-TAGTCAGGCCAGCCGGTTAGGCTGCCACCGAAGGTTGGTAGACGGTGCT GCCTGCGACCAACCCCAGGAGGACTGGGTAAACATGACAGAAATACGAACG AAACTAACGCGCAAAGATCTTTTTTT-3′	3b S21	MVE xr2
	TrmS-spacer_MVE_xrRNA1-tQ	5′-CTCGAGGTGAGCAAGGGCGAGGAGCTGTTCACCGGGGTTGGTGCCCATC CTGGTGGACTTGATAGTCAGGCCAGCCGGTTAGGCTGCCACCGAAGGTTGG TAGACGGTGCTGCCTGCGACCAACCCCAGGAGGACTGGGTAAACATGACAG AAATACGAACGAAACTAACGCGCAAAGATCTTTTTTT-3′	S21	xr3
	TrmS-MVE_xrRNA_element-tQ	5′-CTCGAGGTGAGCAAGGGCGAGGAGCTGTTCACCGGGGTGGTGCCCATCC TGGTGGACTTGATAGTCAGGCCAGCCGGTTAGGCTGCCACCGAAGGTTGGT AGACGGTGCTGCCTGCGACCAACCCCAGGAGGACTGGGTTACCAAAGCTGA TTCTCCACGGTTGGAAAGCCTCCCAGAACCGTCTCGGAAGAGGAGTCCCTG CCAACAATGGAGATGAAGCCCGTGTCAGATCGCGAAAGCGCCACTTCGCCG AGGAGTGCAATCTGTGAGGCCCCAGGAGGACTGGGTAAACAGTCGACCCGG GCGGCCGCAAACATGACAGAAATACGAACGAAACTAACGCGCAAAGATCTT TTTTT-3′	S21	xr4
b	**WNV xrRNAs**			
	TrmS-WNV_xrRNA1_truncate-tQ	5′-AGTCAGGCCAGATTAATGCTGCCACCGGAAGTTGAGTAGACGGTGCTGC CTGCGGCTCAACAAACATGACAGAAATACGAACGAAACTAACGCGCAAAGA TCTTTTTTT-3′	S21	xr5
	TrmS-WNV_xrRNA1-tQ	5′-AGTCAGGCCAGATTAATGCTGCCACCGGAAGTTGAGTAGACGGTGCTGC CTGCGGCTCAACCCCAGGAGGACTGGGTAAACATGACAGAAATACGAACGA AACTAACGCGCAAAGATCTTTTTTT-3′	3b S21	WNV xr6
	TrmS-WNV_xrRNA1_xrRNA2-tQ	5′-AGTCAGGCCAGATTAATGCTGCCACCGGAAGTTGAGTAGACGGTGCTGC CTGCGGCTCAACCCCAGGAGGACTGGGTGACCAAAGCTGCGAGGTGATCCA CGTAAGCCCTCAGAACCGTCTCGGAAGGAGGACCCCACGTGCTTTAGCCTC AAAGCCCAGTGTCAGACCACACTTTAATGTGCCACTCTGCGGAGAGTGCAG TCTGCGATAGTGCCCCAGGTGGACTGGGTAAACATGACAGAAATACGAACG AAACTAACGCGCAAAGATCTTTTTTT-3′	S21	xr7
c	**Zika xrRNAs**			
	TrmS-ZIKV_xrRNA1_truncate-tQ	5′-TGTCAGGCCTGCTAGTCAGCCACAGTTTGGGGAAAGCTGTGCAGCCTGT AACCCCCCCAGGAGAAAACATGACAGAAATACGAACGAAACTAACGCGCAA AGATCTTTTTTT-3′	S21	xr8
	TrmS-ZIKV_xrRNA1-tQ	5′-TGTCAGGCCTGCTAGTCAGCCACAGTTTGGGGAAAGCTGTGCAGCCTGT AACCCCCCCAGGAGAAGCTGGGAAACCAAGCTAAACATGACAGAAATACGA ACGAAACTAACGCGCAAAGATCTTTTTTT-3′	3b S21	Zika xr9
	TrmS-ZIKV_xrRNA1_xrRNA2-tQ	5′-TGTCAGGCCTGCTAGTCAGCCACAGTTTGGGGAAAGCTGTGCAGCCTGT AACCCCCCCAGGAGAAGCTGGGAAACCAAGCTCATAGTCAGGCCGAGAACG CCATGGCACGGAAGAAGCCATGCTGCCTGAAACATGACAGAAATACGAACG AAACTAACGCGCAAAGATCTTTTTTT-3′	S21	xr10
d	**Dengue xrRNA**			
	TrmS-Dengue4_xrRNA-tQ‡	5′-AGTCAGGCCACTTGTGCCACGGTTTGAGCAAACCGTGCTGCCTGTAGCT CCGCCAATAATGGGAGGCGTAAACATGACAGAAATACGAACGAAACTAACG CGCAAAGATCTTTTTTT-3′	3b S21	Dengue xr11
e	**YF xrRNA**			
	TrmS-YF_xrRNA-tQ	5′-TGTCAGCCCAGAACCCCACACGAGTTTTGCCACTGCTAAGCTGTGAGGC AGTGCAGGCTGGGACAGCCGACCTCCAGGTTGCGAAAAACCTGGTAAACAT GACAGAAATACGAACGAAACTAACGCGCAAAGATCTTTTTTT-3′	3b S21	YF xr12

Table S7: Sequences for terminator switch trigger X_Q with different xrRNA variants at the 5′ end. Nucleotides shaded lavender are constrained by an xrRNA sequence from: (a) Murray Valley encephalitis (MVE, NC_000943.1),[1,2] (b) West Nile virus (WNV, NC_001563.2),[1] (c) Zika (NC_012532.1),[1] (d) Dengue (Dengue 4, NC_002640.1),[1] (e) Yellow fever (YF, NC_002031.1).[1] Nucleotides shaded blue are designed as described in Section S1.2. The C nucleotide shaded black is a cloning artifact. Nucleotides shaded tan are constrained by the hU6 terminator sequence.[16]

‡"TrmS-Dengue4_xrRNA-tQ" is the same trigger as "TrmS-xr-tQ" of Table S5d.

Name	Sequence	Figure	Legend
xr-P1-g	5′–AGTCAGGCCACTTGTGCCACGGTTTGAGCAAACCGTGCTGCCTGTAGCT CCGCCAATAATGGGAGGCGTGAGTCGCGTGTAGCGAAGCAGTTTTAGAGCT AGAAATAGCAAGTTAAAATAAGGCTAGTCCGTTATCAACTTGAAAAAGTGG CACCGAGTCGGTGCTTTTTTT–3′	S22a	xr11-gRNA
xr-spacer-P1-g	5′–AGTCAGGCCACTTGTGCCACGGTTTGAGCAAACCGTGCTGCCTGTAGCT CCGCCAATAATGGGAGGCGTGTCCCATTAAGTACCATTCCGAGTCGCGTGT AGCGAAGCAGTTTTAGAGCTAGAAATAGCAAGTTAAAATAAGGCTAGTCCG TTATCAACTTGAAAAAGTGGCACCGAGTCGGTGCTTTTTTT–3′	S22a	xr11-spacer-gRNA
xr-TrmS-cgQ	5′–AGTCAGGCCACTTGTGCCACGGTTTGAGCAAACCGTGCTGCCTGTAGCT CCGCCAATAATGGGAGGCGTGAGTCGCGTGTAGCGAAGCAGTTTTAGAGCT AGAAATAGCAAGTTAAAATAAGGCTAGTCCGATCTTTGCGCGTTAGTTTCG TTCGTATTTCTGTCATGTTTGCGCGGCACCGAGTCGGTGCTTTTTTT–3′	S22a	xr11-cgRNA Q

Table S8: cgRNA/gRNA sequences tested with an xrRNA at the 5′-end. Nucleotides shaded lavender are constrained by the xrRNA sequence (xr11) derived from the Dengue virus type 4 (Dengue 4, NC_002640.1).[1] Nucleotides shaded red are a spacer sequence designed to be unstructured. Nucleotides shaded orange are constrained by the target binding site on the reporter plasmid. Nucleotides shaded gray are constrained by dCas9. Nucleotides shaded tan are constrained by the hU6 terminator sequence.[16] Nucleotides shaded blue are designed as described in Section S1.2.

Name	Sequence	Figure	Legend
G-xr-TrmS-tQ	5′–GAGTCAGGCCACTTGTGCCACGGTTTGAGCAAACCGTGCTGCCTGTAGCT CCGCCAATAATGGGAGGCGTAAACATGACAGAAATACGAACGAAACTAACG CGCAAAGATCTTTTTTT–3′	S22b	G-xr11-X_Q
G-TrmS-tQ-xr	5′–GAAACATGACAGAAATACGAACGAAACTAACGCGCAAAGATAGTCAGGC CACTTGTGCCACGGTTTGAGCAAACCGTGCTGCCTGTAGCTCCGCCAATAA TGGGAGGCGTCTTTTTTT–3′	S22b	G-X_Q-xr11
G-TrmS-tQ-rev_xr	5′–GAAACATGACAGAAATACGAACGAAACTAACGCGCAAAGATTGCGGAGG GTAATAACCGCCTCGATGTCCGTCGTGCCAAACGAGTTTGGCACCGTGTTC ACCGGACTGACTTTTTTT–3′	S22b	G-X_Q-xr11rev

Table S9: Sequences of terminator switch trigger X_Q with an xrRNA at various locations The G shaded red potentially enhances the strength of the transcription start site.[17] Nucleotides shaded lavender are constrained by the xrRNA sequence (xr11) derived from the Dengue virus type 4 (Dengue 4, NC_002640.1).[1] Nucleotides shaded blue are designed as described in Section S1.2. The C nucleotide shaded black is a cloning artifact. Nucleotides shaded tan are constrained by the hU6 terminator sequence.[16]

Name	Sequence	Figure	Legend
P1-g_−8nt	5′–GAGTCGCGTGTAGCGAAGCAGTTTTAGAGCTAGAAATAGCAAGTTAAAAT AAGGCTAGTCCGTTATCAACTTGAAAAAGTGGCACCGCTTTTTTT–3′	S26	8nt deletion
P1-g_−23nt	5′–GAGTCGCGTGTAGCGAAGCAGTTTTAGAGCTAGAAATAGCAAGTTAAAAT AAGGCTAGTCCGTTATCAACTTCTTTTTTT–3′	S26	23nt deletion
P1-g_−32nt	5′–GAGTCGCGTGTAGCGAAGCAGTTTTAGAGCTAGAAATAGCAAGTTAAAAT AAGGCTAGTCCGTCTTTTTTT–3′	S26	32nt deletion
P1-g_−45nt	5′–GAGTCGCGTGTAGCGAAGCAGTTTTAGAGCTAGAAATAGCAAGTTAAAAT CTTTTTTT–3′	S26	45nt deletion

Table S10: Sequences of truncated standard P1 gRNAs. Nucleotides shaded orange are constrained by the target binding site on the reporter plasmid. Nucleotides shaded gray are constrained by dCas9. The C nucleotide shaded black is a cloning artifact. Nucleotides shaded tan are constrained by the hU6 terminator sequence.[16]

	Name	Sequence	Figure	Legend
a	**cgRNAs**			
	STS-cgβ_40	5′–AGTCGCGTGTAGCGAAGCAGTTTAAGAGCTATGCTGGAAACAGCATAGC AAGTTTAAATAAGGCTAGTCCGTTATCACATATCCCATCCACCTCCACCTC CACCTCCACATTCCCACCTTTTTTTT–3′	S27b	|d| = 40
	STS-cgβ_30	5′–AGTCGCGTGTAGCGAAGCAGTTTAAGAGCTATGCTGGAAACAGCATAGC AAGTTTAAATAAGGCTAGTCCGTTATCACATATCCCATCCACCTCCACCTC CACCTCCCTTTTTTT–3′	S27b	|d| = 30
	STS-cgβ_20	5′–AGTCGCGTGTAGCGAAGCAGTTTAAGAGCTATGCTGGAAACAGCATAGC AAGTTTAAATAAGGCTAGTCCGTTATCACATATCCCATCCACCTCCACCTT TTTTT–3′	S27b	|d| = 20
	STS-cgβ_10	5′–AGTCGCGTGTAGCGAAGCAGTTTAAGAGCTATGCTGGAAACAGCATAGC AAGTTTAAATAAGGCTAGTCCGTTATCACATATCCCATCTTTTTTT–3′	S27b	|d| = 10
b	**Triggers**			
	STS-tβ_40	5′–AGTCAGGCCACTTGTGCCACGGTTTGAGCAAACCGTGCTGCCTGTAGCT CCGCCAATAATGGGAGGCGTGTGGGAATGTGGAGGTGGAGGTGGAGGTGGA TGGGATATGGGCACCGAGTCGGTGCTTTTTTT–3′	S27b	Trigger X_{40}
	STS-tβ_30	5′–AGTCAGGCCACTTGTGCCACGGTTTGAGCAAACCGTGCTGCCTGTAGCT CCGCCAATAATGGGAGGCGTGGAGGTGGAGGTGGAGGTGGATGGGATATGG GCACCGAGTCGGTGCTTTTTTT–3′	S27b	Trigger X_{30}
	STS-tβ_20	5′–AGTCAGGCCACTTGTGCCACGGTTTGAGCAAACCGTGCTGCCTGTAGCT CCGCCAATAATGGGAGGCGTGTGGAGGTGGATGGGATATGGGCACCGAGTC GGTGCTTTTTTTT–3′	S27b	Trigger X_{20}
	STS-tβ_10	5′–AGTCAGGCCACTTGTGCCACGGTTTGAGCAAACCGTGCTGCCTGTAGCT CCGCCAATAATGGGAGGCGTATGGGATATGGGCACCGAGTCGGTGCTTTTT TT–3′	S27b	Trigger X_{10}

Table S11: Split-terminator switch sequences (OFF→ON logic) with domain $|\mathbf{d}| = \{40, 30, 20, 10\}$ nt. NUPACK was used to design a split-terminator switch with |d| = 40 nt, from which truncated versions with $|\mathrm{d}| = \{30, 20, 10\}$ nt were also made for experimental study. Nucleotides shaded orange are constrained by the target binding site on the reporter plasmid. Nucleotides shaded gray are constrained by dCas9. Nucleotides shaded blue are designed as described in Section S1.2. The C nucleotide shaded black is a cloning artifact. Nucleotides shaded tan are constrained by the hU6 terminator sequence.[16] Nucleotides shaded lavender are constrained by the xrRNA sequence (xr11) derived from the Dengue virus type 4 (Dengue 4, NC_002640.1).[1]

	Name	Sequence	Figure	Legend
a	**cgRNAs and triggers: |d| = 10nt**			
	STS-cgM_10	5′-GAGTCGCGTGTAGCGAAGCAGTTTAAGAGCTATGCTGGAAACAGCATA	S28c	cgRNA
		GCAAGTTTAAATAAGGCTAGTCCGTTATCAGCACATCCCACTTTTTTT-3′	S28d	cgRNA M
			S29b	10nt cgRNA M
	STS-cgN_10	5′-GAGTCGCGTGTAGCGAAGCAGTTTAAGAGCTATGCTGGAAACAGCATAGC	S28d	cgRNA N
		AAGTTTAAATAAGGCTAGTCCGTTATCAGGCCAGGTTCCTTTTTTT-3′	S29b	10nt cgRNA N
	STS-cgO_10	5′-GAGTCGCGTGTAGCGAAGCAGTTTAAGAGCTATGCTGGAAACAGCATAGC	S28d	cgRNA O
		AAGTTTAAATAAGGCTAGTCCGTTATCACCCAGAACACCTTTTTTT-3′	S29b	10nt cgRNA O
	STS-xr-tM_10	5′-AGTCAGGCCACTTGTGCCACGGTTTGAGCAAACCGTGCTGCCTGTAGCTC	S28c	Trigger
		CGCCAATAATGGGAGGCGTTGGGATGTGCGGCACCGAGTCGGTGCTTTTTT	S28d	Trigger X_M
		T-3′	S29b	10nt Trigger X_M
	STS-xr-tN_10	5′-AGTCAGGCCACTTGTGCCACGGTTTGAGCAAACCGTGCTGCCTGTAGCTC	S28d	Trigger X_N
		CGCCAATAATGGGAGGCGTGAACCTGGCCGGCACCGAGTCGGTGCTTTTTT	S29b	10nt Trigger X_N
		T-3′		
	STS-xr-tO_10	5′-AGTCAGGCCACTTGTGCCACGGTTTGAGCAAACCGTGCTGCCTGTAGCTC	S28d	Trigger X_O
		CGCCAATAATGGGAGGCGTGTGTTCTGGGGGCACCGAGTCGGTGCTTTTTT	S29b	10nt Trigger X_O
		T-3′		
b	**cgRNAs and triggers: |d| = 8nt**			
	STS-cgM_8	5′-GAGTCGCGTGTAGCGAAGCAGTTTAAGAGCTATGCTGGAAACAGCATAGC	S29b	8nt cgRNA M
		AAGTTTAAATAAGGCTAGTCCGTTATCAGCACATCCCTTTTTTT-3′		
	STS-cgN_8	5′-GAGTCGCGTGTAGCGAAGCAGTTTAAGAGCTATGCTGGAAACAGCATAGC	S29b	8nt cgRNA N
		AAGTTTAAATAAGGCTAGTCCGTTATCAGGCCAGGTCTTTTTTT-3′		
	STS-cgO_8	5′-GAGTCGCGTGTAGCGAAGCAGTTTAAGAGCTATGCTGGAAACAGCATAGC	S29b	8nt cgRNA O
		AAGTTTAAATAAGGCTAGTCCGTTATCACCCAGAACCTTTTTTT-3′		
	STS-xr-tM_8	5′-AGTCAGGCCACTTGTGCCACGGTTTGAGCAAACCGTGCTGCCTGTAGCTC	S29b	8nt Trigger X_M
		CGCCAATAATGGGAGGCGTGGATGTGCGGCACCGAGTCGGTGCTTTTTTT-3′		
	STS–xr-tN_8	5′-AGTCAGGCCACTTGTGCCACGGTTTGAGCAAACCGTGCTGCCTGTAGCTC	S29b	8nt Trigger X_N
		CGCCAATAATGGGAGGCGTACCTGGCCGGCACCGAGTCGGTGCTTTTTTT-3′		
	STS-xr-tO_8	5′-AGTCAGGCCACTTGTGCCACGGTTTGAGCAAACCGTGCTGCCTGTAGCTC	S29b	8nt Trigger X_O
		CGCCAATAATGGGAGGCGTGTTCTGGGGGCACCGAGTCGGTGCTTTTTTT-3′		
c	**cgRNAs and triggers: |d| = 6nt**			
	STS-cgM_6	5′-GAGTCGCGTGTAGCGAAGCAGTTTAAGAGCTATGCTGGAAACAGCATAGC	S29b	6nt cgRNA M
		AAGTTTAAATAAGGCTAGTCCGTTATCAGCACATCTTTTTTT-3′		
	STS-cgN_6	5′-GAGTCGCGTGTAGCGAAGCAGTTTAAGAGCTATGCTGGAAACAGCATAGC	S29b	6nt cgRNA N
		AAGTTTAAATAAGGCTAGTCCGTTATCAGGCCAGCTTTTTTT-3′		
	STS-cgO_6	5′-GAGTCGCGTGTAGCGAAGCAGTTTAAGAGCTATGCTGGAAACAGCATAGC	S29b	6nt cgRNA O
		AAGTTTAAATAAGGCTAGTCCGTTATCACCCAGACTTTTTTT-3′		
	STS-xr-tM_6	5′-AGTCAGGCCACTTGTGCCACGGTTTGAGCAAACCGTGCTGCCTGTAGCTC	S29b	6nt Trigger X_M
		CGCCAATAATGGGAGGCGTATGTGCGGCACCGAGTCGGTGCTTTTTTT-3′		
	STS-xr-tN_6	5′-AGTCAGGCCACTTGTGCCACGGTTTGAGCAAACCGTGCTGCCTGTAGCTC	S29b	6nt Trigger X_N
		CGCCAATAATGGGAGGCGTCTGGCCGGCACCGAGTCGGTGCTTTTTTT-3′		
	STS-xr-tO_6	5′-AGTCAGGCCACTTGTGCCACGGTTTGAGCAAACCGTGCTGCCTGTAGCTC	S29b	6nt Trigger X_O
		CGCCAATAATGGGAGGCGTTCTGGGGGCACCGAGTCGGTGCTTTTTTT-3′		

Table S12: Split-terminator switch sequences (OFF→ON logic) with domain $|d| = \{10, 8, 6, 4\}$ nt. NUPACK was used to design a library of split-terminator switches with |d| = 10 nt, from which truncated versions with $|d| = \{8, 6, 4\}$ nt were also made for experimental study. The sequences with $|d| = 4$ nt are displayed in Table S6. Nucleotides shaded orange are constrained by the target binding site on the reporter plasmid. Nucleotides shaded gray are constrained by dCas9. Nucleotides shaded blue are designed as described in Section S1.2. The C nucleotide shaded black is a cloning artifact. Nucleotides shaded tan are constrained by the hU6 terminator sequence.[16] Nucleotides shaded lavender are constrained by the xrRNA sequence (xr11) derived from the Dengue virus type 4 (Dengue 4, NC_002640.1).[1]

S3 Representative plasmid maps and annotated sequences

Table S13 describes the plasmid constructs used for main text Figures 3-5. Representative plasmid maps and annotated sequences are provided in Figures S8–S13. Plasmids for additional studies were constructed analogously.

	Name	Parts	Figures	Legend
a	**Plasmids used in cgRNA studies**			
	SP-dCas9-VPR	Addgene plasmid #63798	3, 4, 5	
	P1-minCMV-PhiYFP	pUC ori; amp-R; P1 binding site–minCMV promoter–PhiYFP–SV40 poly(A) signal	3, 4, 5	
	pNT-g	pUC ori; amp-R; hU6 promoter–NT-g; PGK promoter–miRFP670–SV40 poly(A) signal	3, 4	No-target gRNA
	pP1-g	pUC ori; amp-R; hU6 promoter–P1-g; PGK promoter–miRFP670–SV40 poly(A) signal	3, 4	Standard gRNA
	pNT-g-FE	pUC ori; amp-R; hU6 promoter–NT-g-FE; PGK promoter–miRFP670–SV40 poly(A) signal	5	No-target gRNA
	pP1-g-FE	pUC ori; amp-R; hU6 promoter–P1-g-FE; PGK promoter–miRFP670–SV40 poly(A) signal	5	Standard gRNA
b	**Terminator switch plasmids (ON→OFF logic)**			
	pTrmS-cgQ	pUC ori; amp-R; hU6 promoter–TrmS-cgQ; PGK promoter–miRFP670–SV40 poly(A) signal	3, 4	cgRNA, cgRNA Q
	pTrmS-cgR	pUC ori; amp-R; hU6 promoter–TrmS-cgR; PGK promoter–miRFP670–SV40 poly(A) signal	4	cgRNA R
	pTrmS-cgS	pUC ori; amp-R; hU6 promoter–TrmS-cgS; PGK promoter–miRFP670–SV40 poly(A) signal	4	cgRNA S
	pTrmS-cgT	pUC ori; amp-R; hU6 promoter–TrmS-cgT; PGK promoter–miRFP670–SV40 poly(A) signal	4	cgRNA T
	pTrmS-40	pUC ori; amp-R; hU6 promoter–TrmS-40; PGK promoter–EBFP2–SV40 poly(A) signal	3c(left)	−Trigger
	pTrmS-tQ	pUC ori; amp-R; hU6 promoter–TrmS-tQ; PGK promoter–EBFP2–SV40 poly(A) signal	3b,c(left)	Trigger
	pTrmS-xr-40	pUC ori; amp-R; hU6 promoter–TrmS-xr-40; PGK promoter–EBFP2–SV40 poly(A) signal	3b 3c(right), 4	No trigger −Trigger
	pTrmS-xr-tQ	pUC ori; amp-R; hU6 promoter–TrmS-xr-tQ; PGK promoter–EBFP2–SV40 poly(A) signal	3b,c(right) 4	Trigger Dengue, Trigger Trigger, Trigger X_Q
	pTrmS-MVE-tQ	pUC ori; amp-R; hU6 promoter–TrmS-MVE_xrRNA1-tQ; PGK promoter–EBFP2–SV40 poly(A) signal	3	Trigger MVE
	pTrmS-WNV-tQ	pUC ori; amp-R; hU6 promoter–TrmS-WNV_xrRNA1-tQ; PGK promoter–EBFP2–SV40 poly(A) signal	3	Trigger WNV
	pTrmS-Zika-tQ	pUC ori; amp-R; hU6 promoter–TrmS-Zika_xrRNA1-tQ; PGK promoter–EBFP2–SV40 poly(A) signal	3	Trigger Zika
	pTrmS-YF-tQ	pUC ori; amp-R; hU6 promoter–TrmS-YF_xrRNA1-tQ; PGK promoter–EBFP2–SV40 poly(A) signal	3	Trigger YF
	pTrmS-xr-tR	pUC ori; amp-R; hU6 promoter–TrmS-xr-tR; PGK promoter–EBFP2–SV40 poly(A) signal	4	Trigger X_R
	pTrmS-xr-tS	pUC ori; amp-R; hU6 promoter–TrmS-xr-tS; PGK promoter–EBFP2–SV40 poly(A) signal	4	Trigger X_S
	pTrmS-xr-tT	pUC ori; amp-R; hU6 promoter–TrmS-xr-tT; PGK promoter–EBFP2–SV40 poly(A) signal	4	Trigger X_T
c	**Split-terminator switch plasmids (OFF→ON logic)**			
	pSTS-cgM	pUC ori; amp-R; hU6 promoter–STS-cgM; PGK promoter–miRFP670–SV40 poly(A) signal	5	cgRNA, cgRNA M
	pSTS-cgN	pUC ori; amp-R; hU6 promoter–STS-cgN; PGK promoter–miRFP670–SV40 poly(A) signal	5	cgRNA N
	pSTS-cgO	pUC ori; amp-R; hU6 promoter–STS-cgO; PGK promoter–miRFP670–SV40 poly(A) signal	5	cgRNA O
	pSTS-19	pUC ori; amp-R; hU6 promoter–STS-19; PGK promoter–EBFP2–SV40 poly(A) signal	5	−Trigger
	pSTS-tM	pUC ori; amp-R; hU6 promoter–STS-tM; PGK promoter–EBFP2–SV40 poly(A) signal	5	Trigger, Trigger X_M
	pSTS-tN	pUC ori; amp-R; hU6 promoter–STS-tN; PGK promoter–EBFP2–SV40 poly(A) signal	5	Trigger X_N
	pSTS-tO	pUC ori; amp-R; hU6 promoter–STS-tO; PGK promoter–EBFP2–SV40 poly(A) signal	5	Trigger X_O

Table S13: Plasmids used for cgRNA studies in HEK 293T cells

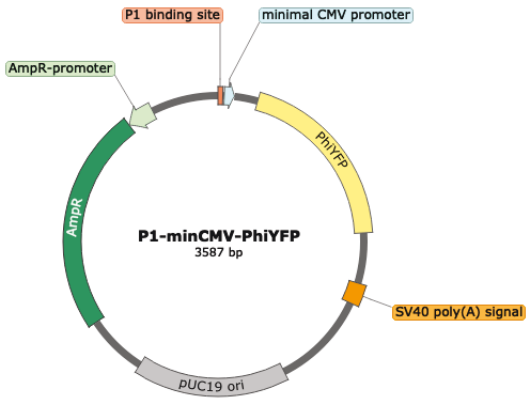

Figure S8: Plasmid map for PhiYFP reporter. Plasmid: P1-minCMV-PhiYFP.

```
AGTCGCGTGTAGCGAAGCAGGGCGAGGTAGGCGTGTACGGTGGGAGGCCTATATAAGCAGAGCTC      65
GTTTAGTGAACCGTCAGATCGCCTGGAGAATTCGCCACCATGGACTACAAGGATGACGACGATAA     130
AACTTCCGGTGGCGGACTGGGTTCCACCATGAGCAGCGGCGCCCTGCTGTTCCACGGCAAGATCC     195
CCTACGTGGTGGAGATGGAGGGCGATGTGGATGGCCACACCTTCAGCATCCGCGGTAAGGGCTAC     260
GGCGATGCCAGCGTGGGCAAGGTGGATGCCCAGTTCATCTGCACCACCGGCGATGTGCCCGTGCC     325
CTGGAGCACCCTGGTGACCACCCTGACCTACGGCGCCCAGTGCTTCGCCAAGTACGGCCCCGAGC     390
TGAAGGATTTCTACAAGAGCTGCATGCCCGATGGCTACGTGCAGGAGCGCACCATCACCTTCGAG     455
GGCGATGGCAATTTCAAGACCCGCGCCGAGGTGACCTTCGAGAATGGCAGCGTGTACAATCGCGT     520
GAAGCTGAATGGCCAGGGCTTCAAGAAGGATGGCCACGTGCTGGGCAAGAATCTGGAGTTCAATT     585
TCACCCCCCACTGCCTGTACATCTGGGGCGATCAGGCCAATCACGGCCTGAAGAGCGCCTTCAAG     650
ATCTGCCACGAGATCGCCGGCAGCAAGGGCGATTTCATCGTGGCCGATCACACCCAGATGAATAC     715
CCCCATCGGCGGCGGCCCCGTGCACGTGCCCGAGTACCACCACATGAGCTACCACGTGAAGCTGA     780
GCAAGGATGTGACCGATCACCGCGATAATATGAGCCTGACGGAGACAGTGCGCGCCGTGGATTGC     845
CGCAAGACCTACCTGTAATAAGAATTCGAGCTCGGTACCCGGGGATCCTCTAGTCAGCTGACGCG     910
TGCTAGCGCGGCCGCATCGATAAGCTTGTCGACGATATCTCTAGAGGATCATAATCAGCCATACC     975
ACATTTGTAGAGGTTTTACTTGCTTTAAAAAACCTCCCACACCTCCCCCTGAACCTGAAACATAA    1040
AATGAATGCAATTGTTGTTGTTAACTTGTTTATTGCAGCTTATAATGGTTACAAATAAAGCAATA    1105
GCATCACAAATTTCACAAATAAAGCATTTTTTTCACTGCCTCGAGCTTCCTCGCTCACTGACTCG    1170
CTGCGCTCGGTCGTTCGGCTGCGGCGAGCGGTATCAGCTCACTCAAAGGCGGTAATAAAGGGCGA    1235
ATTCCAGCACACTGGCGGCCGTTACTAGTGGATCCGAGCTCGGTACCAGGCTAGGTGGAGGCTCA    1300
GTGATGATAAGTCTGCGATGGTGGATGCATGTGTCATGGTCATAGCTGTTTCCTGTGTGAAATTG    1365
TTATCCGCTCAGAGGGCACAATCCTATTCCGCGCTATCCGACAATCTCCAAGACATTAGGTGGAG    1430
TTCAGTTCGGCGTATGGCATATGTCGCTGGAAAGAACATGTGAGCAAAAGGCCAGCAAAAGGCCA    1495
GGAACCGTAAAAAGGCCGCGTTGCTGGCGTTTTTCCATAGGCTCCGCCCCCCTGACGAGCATCAC    1560
AAAAATCGACGCTCAAGTCAGAGGTGGCGAAACCCGACAGGACTATAAAGATACCAGGCGTTTCC    1625
CCCTGGAAGCTCCCTCGTGCGCTCTCCTGTTCCGACCCTGCCGCTTACCGGATACCTGTCCGCCT    1690
TTCTCCCTTCGGGAAGCGTGGCGCTTTCTCATAGCTCACGCTGTAGGTATCTCAGTTCGGTGTAG    1755
GTCGTTCGCTCCAAGCTGGGCTGTGTGCACGAACCCCCCGTTCAGCCCGACCGCTGCGCCTTATC    1820
CGGTAACTATCGTCTTGAGTCCAACCCGGTAAGACACGACTTATCGCCACTGGCAGCAGCCACTG    1885
GTAACAGGATTAGCAGAGCGAGGTATGTAGGCGGTGCTACAGAGTTCTTGAAGTGGTGGCCTAAC    1950
TACGGCTACACTAGAAGAACAGTATTTGGTATCTGCGCTCTGCTGAAGCCAGTTACCTTCGGAAA    2015
AAGAGTTGGTAGCTCTTGATCCGGCAAACAAACCACCGCTGGTAGCGGTGGTTTTTTTGTTTGCA    2080
AGCAGCAGATTACGCGCAGAAAAAAAGGATCTCAAGAAGATCCTTTGATCTTTTCTACGGGGTCT    2145
GACGCTCTATTCAACAAAGCCGCCGTCCCGTCAAGTCAGCGTAAATGGGTAGGGGGCTTCAAATC    2210
GTCCTCGTGATACCAATTCGGAGCCTGCTTTTTTGTACAAACTTGTTGATAATGGCAATTCAAGG    2275
ATCTTCACCTAGATCCTTTTAAATTAAAAATGAAGTTTTAAATCAATCTAAAGTATATATGAGTA    2340
AACTTGGTCTGACAGTTACCAATGCTTAATCAGTGAGGCACCTATCTCAGCGATCTGTCTATTTC    2405
GTTCATCCATAGTTGCCTGACTCCCCGTCGTGTAGATAACTACGATACGGGAGGGCTTACCATCT    2470
GGCCCCAGTGCTGCAATGATACCGCGAGAGCCACGCTCACCGGCTCCAGATTTATCAGCAATAAA    2535
CCAGCCAGCCGGAAGGGCCGAGCGCAGAAGTGGTCCTGCAACTTTATCCGCCTCCATCCAGTCTA    2600
TTAATTGTTGCCGGGAAGCTAGAGTAAGTAGTTCGCCAGTTAATAGTTTGCGCAACGTTGTTGCC    2665
ATTGCTACAGGCATCGTGGTGTCACGCTCGTCGTTTGGTATGGCTTCATTCAGCTCCGGTTCCCA    2730
ACGATCAAGGCGAGTTACATGATCCCCCATGTTGTGCAAAAAAGCGGTTAGCTCCTTCGGTCCTC    2795
CGATCGTTGTCAGAAGTAAGTTGGCCGCAGTGTTATCACTCATGGTTATGGCAGCACTGCATAAT    2860
TCTCTTACTGTCATGCCATCCGTAAGATGCTTTTCTGTGACTGGTGAGTACTCAACCAAGTCATT    2925
CTGAGAATAGTGTATGCGGCGACCGAGTTGCTCTTGCCCGGCGTCAATACGGGATAATACCGCGC    2990
CACATAGCAGAACTTTAAAAGTGCTCATCATTGGAAAACGTTCTTCGGGGCGAAAACTCTCAAGG    3055
ATCTTACCGCTGTTGAGATCCAGTTCGATGTAACCCACTCGTGCACCCAACTGATCTTCAGCATC    3120
TTTTACTTTCACCAGCGTTTCTGGGTGAGCAAAAACAGGAAGGCAAAATGCCGCAAAAAAGGGAA    3185
TAAGGGCGACACGGAAATGTTGAATACTCATACTCTTCCTTTTTCAATATTATTGAAGCATTTAT    3250
CAGGGTTATTGTCTCATGAGCGGATACATATTTGAATGTATTTAGAAAAATAAACAAATAGGGGT    3315
TCCGCGCACATTTCCCCGAAAAGTGCCAGATACCTGAAACAAAACCCATCGTACGGCCAAGGAAG    3380
TCTCCAATAACTGTGATCCACCACAAGCGCCAGGGTTTTCCCAGTCACGACGTTGTAAAACGACG    3445
GCCAGTCATGCATAATCCGCACGCATCTGGAATAAGGAAGTGCCATTCCGCCTGACCTTCTAGAT    3510
GCATGCTCGAGCGGCCGCCAGTGTGATGGATATCTGCAGAATTCGCCCTTGCGACGTAGGGATAA    3575
CAGGGTAATAGT ... 3587
```

Figure S9: Annotated plasmid sequence for PhiYFP reporter. Plasmid: P1-minCMV-PhiYFP.

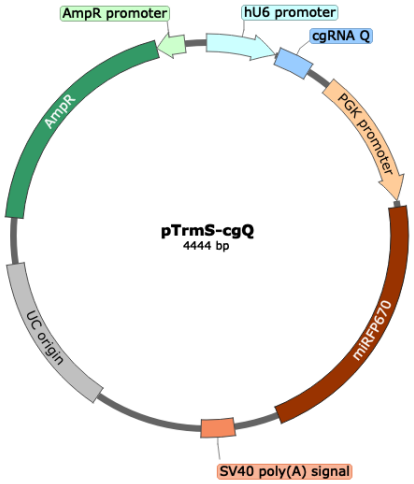

Figure S10: Representative plasmid map for cgRNA plasmids in HEK 293T cells. Plasmid: pTrmS-cgQ for cgRNA Q.

```
AAGGTCGGGCAGGAAGAGGGCCTATTTCCCATGATTCCTTCATATTTGCATATACGATACAAGGC      65
TGTTAGAGAGATAATTAGAATTAATTTGACTGTAAACACAAAGATATTAGTACAAAATACGTGAC     130
GTAGAAAGTAATAATTTCTTGGGTAGTTTGCAGTTTTAAAATTATGTTTTAAAATGGACTATCAT     195
ATGCTTACCGTAACTTGAAAGTATTTCGATTTCTTGGCTTTATATATCTTGTGGAAAGGACGAAA     260
CACCGAGTCGCGTGTAGCGAAGCAGTTTTAGAGCTAGAAATAGCAAGTTAAAATAAGGCTAGTCC     325
GATCTTTGCGCGTTAGTTTCGTTCGTATTTCTGTCATGTTTGCGCGGCACCGAGTCGGTGCTTTT     390
TTTCTAGAAAGCTTGTCTTCGAGCTCCTCGAGGAAGACCTCTAGACCCAGCTTTCTTGTACAAAG     455
TTGGCATTAGACGTCGAGGAATTCTACCGGGTAGGGGAGGCGCTTTTCCCAAGGCAGTCTGGAGC     520
ATGCGCTTTAGCAGCCCCGCTGGGCACTTGGCGCTACACAAGTGGCCTCTGGCCTCGCACACATT     585
CCACATCCACCGGTAGGCGCCAACCGGCTCCGTTCTTTGGTGGCCCCTTCGCGCCACCTTCTACT     650
CCTCCCCTAGTCAGGAAGTTCCCCCCCGCCCCGCAGCTCGCGTCGTGCAGGACGTGACAAATGGA     715
AGTAGCACGTCTCACTAGTCTCGTGCAGATGGACAGCACCGCTGAGCAATGGAAGCGGGTAGGCC     780
TTTGGGGCAGCGGCCAATAGCAGCTTTGCTCCTTCGCTTTCTGGGCTCAGAGGCTGGGAAGGGGT     845
GGGTCCGGGGGCGGGCTCAGGGGCGGGCTCAGGGGCGGGGCGGGCGCCCGAAGGTCCTCCGGAGG     910
CCCGGCATTCTGCACGCTTCAAAAGCGCACGTCTGCCGCGCTGTTCTCCTCTTCCTCATCTCCGG     975
GCCTTTCGACCTGCATCCCAAGCTTGCCACCATGGTAGCAGGTCATGCCTCTGGCAGCCCCGCAT    1040
TCGGGACCGCCTCTCATTCGAATTGCGAACATGAAGAGATCCACCTCGCCGGCTCGATCCAGCCG    1105
CATGGCGCGCTTCTGGTCGTCAGCGAACATGATCATCGCGTCATCCAGGCCAGCGCCAACGCCGC    1170
GGAATTTCTGAATCTCGGAAGCGTACTCGGCGTTCCGCTCGCCGAGATCGACGGCGATCTGTTGA    1235
TCAAGATCCTGCCGCATCTCGATCCCACCGCCGAAGGCATGCCGGTCGCGGTGCGCTGCCGGATC    1300
GGCAATCCCTCTACGGAGTACTGCGGTCTGATGCATCGGCCTCCGGAAGGCGGGCTGATCATCGA    1365
ACTCGAACGTGCCGGCCCGTCGATCGATCTGTCAGGCACGCTGGCGCCGGCGCTGGAGCGGATCC    1430
GCACGGCGGGTTCACTGCGCGCGCTGTGCGATGACACCGTGCTGCTGTTTCAGCAGTGCACCGGC    1495
TACGACCGGGTGATGGTGTATCGTTTCGATGAGCAAGGCCACGGCCTGGTATTCTCCGAGTGCCA    1560
TGTGCCTGGGCTCGAATCCTATTTCGGCAACCGCTATCCGTCGTCGACTGTCCCGCAGATGGCGC    1625
GGCAGCTGTACGTGCGGCAGCGCGTCCGCGTGCTGGTCGACGTCACCTATCAGCCGGTGCCGCTG    1690
GAGCCGCGGCTGTCGCCGCTGACCGGGCGCGATCTCGACATGTCGGGCTGCTTCCTGCGCTCGAT    1755
GTCGCCGTGCCATCTGCAGTTCCTGAAGGACATGGGCGTGCGCGCCACCCTGGCGGTGTCGCTGG    1820
TGGTCGGCGGCAAGCTGTGGGGCCTGGTTGTCTGTCACCATTATCTGCCGCGCTTCATCCGTTTC    1885
GAGCTGCGGGCGATCTGCAAACGGCTCGCCGAAAGGATCGCGACGCGGATCACCGCGCTTGAGAG    1950
CTAAGTACCACTAGTACCGGTAGATATCAGCCATGGCTTCCCGCCGGCGGTGGCGGCGCAGGATG    2015
ATGGCACGCTGCCCATGTCTTGTGCCCAGGAGAGCGGGATGGACCGTCACCCTGCAGCCTGTGCT    2080
TCTGCTAGGATCAATGTGTAGGCTAGTCGAGCAGACATGATAAGATACATTGATGAGTTTGGACA    2145
AACCACAACTAGAATGCAGTGAAAAAAATGCTTTATTTGTGAAATTTGTGATGCTATTGCTTTAT    2210
TTGTAACCATTATAAGCTGCAATAAACAAGTTAACAACAACAATTGCATTCATTTTATGTTTCAG    2275
GTTCAGGGGGAGATGTGGGAGGTTTTTTAAAGCAAGTAAAACCTCTACAAATGTGGTAAAATCCG    2340
ATAAGGATCGATCCGGGCTGGCGTAATAGCGAAGAGGCCCGCACCGATCGCCCTTCCCAACAGTT    2405
GCCTGCATTAATGAATCGGCCAACGCGCGGGGAGAGGCGGTTTGCGTATTGGGCGCTCTTCCGCT    2470
TCCTCGCTCACTGACTCGCTGCGCTCGGTCGTTCGGCTGCGGCGAGCGGTATCAGCTCACTCAAA    2535
GGCGGTAATACGGTTATCCACAGAATCAGGGGATAACGCAGGAAAGAACATGTGAGCAAAAGGCC    2600
AGCAAAAGGCCAGGAACCGTAAAAAGGCCGCGTTGCTGGCGTTTTTCCATAGGCTCCGCCCCCCT    2665
GACGAGCATCACAAAAATCGACGCTCAAGTCAGAGGTGGCGAAACCCGACAGGACTATAAAGATA    2730
CCAGGCGTTTCCCCCTGGAAGCTCCCTCGTGCGCTCTCCTGTTCCGACCCTGCCGCTTACCGGAT    2795
ACCTGTCCGCCTTTCTCCCTTCGGGAAGCGTGGCGCTTTCTCATAGCTCACGCTGTAGGTATCTC    2860
AGTTCGGTGTAGGTCGTTCGCTCCAAGCTGGGCTGTGTGCACGAACCCCCCGTTCAGCCCGACCG    2925
CTGCGCCTTATCCGGTAACTATCGTCTTGAGTCCAACCCGGTAAGACACGACTTATCGCCACTGG    2990
CAGCAGCCACTGGTAACAGGATTAGCAGAGCGAGGTATGTAGGCGGTGCTACAGAGTTCTTGAAG    3055
TGGTGGCCTAACTACGGCTACACTAGAAGAACAGTATTTGGTATCTGCGCTCTGCTGAAGCCAGT    3120
TACCTTCGGAAAAAGAGTTGGTAGCTCTTGATCCGGCAAACAAACCACCGCTGGTAGCGGTTTTT    3185
TTGTTTGCAAGCAGCAGATTACGCGCAGAAAAAAAGGATCTCAAGAAGATCCTTTGATCTTTTCT    3250
ACGGGGTCTGACGCTCAGTGGAACGAAAACTCACGTTAAGGGATTTTGGTCATGAGATTATCAAA    3315
AAGGATCTTCACCTAGATCCTTTTAAATTAAAAATGAAGTTTTAAATCAATCTAAAGTATATATG    3380
AGTAAACTTGGTCTGACAGTTACCAATGCTTAATCAGTGAGGCACCTATCTCAGCGATCTGTCTA    3445
TTTCGTTCATCCATAGTTGCCTGACTCCCCGTCGTGTAGATAACTACGATACGGGAGGGCTTACC    3510
ATCTGGCCCCAGTGCTGCAATGATACCGCGCGACCCACGCTCACCGGCTCCAGATTTATCAGCAA    3575
TAAACCAGCCAGCCGGAAGGGCCGAGCGCAGAAGTGGTCCTGCAACTTTATCCGCCTCCATCCAG    3640
TCTATTAATTGTTGCCGGGAAGCTAGAGTAAGTAGTTCGCCAGTTAATAGTTTGCGCAACGTTGT    3705
TGCCATTGCTACAGGCATCGTGGTGTCACGCTCGTCGTTTGGTATGGCTTCATTCAGCTCCGGTT    3770
CCCAACGATCAAGGCGAGTTACATGATCCCCCATGTTGTGCAAAAAAGCGGTTAGCTCCTTCGGT    3835
CCTCCGATCGTTGTCAGAAGTAAGTTGGCCGCAGTGTTATCACTCATGGTTATGGCAGCACTGCA    3900
TAATTCTCTTACTGTCATGCCATCCGTAAGATGCTTTTCTGTGACTGGTGAGTACTCAACCAAGT    3965
CATTCTGAGAATAGTGTATGCGGCGACCGAGTTGCTCTTGCCCGGCGTCAATACGGGATAATACC    4030
GCGCCACATAGCAGAACTTTAAAAGTGCTCATCATTGGAAAACGTTCTTCGGGGCGAAAACTCTC    4095
AAGGATCTTACCGCTGTTGAGATCCAGTTCGATGTAACCCACTCGTGCACCCAACTGATCTTCAG    4160
CATCTTTTACTTTCACCAGCGTTTCTGGGTGAGCAAAAACAGGAAGGCAAAATGCCGCAAAAAAG    4225
GGAATAAGGGCGACACGGAAATGTTGAATACTCATACTCTTCCTTTTTCAATATTATTGAAGCAT    4290
TTATCAGGGTTATTGTCTCATGAGCGGATACATATTTGAATGTATTTAGAAAAATAAACAAATAG    4355
GGGTTCCGCGCACATTTCCCCGAAAAGTGCCACCTTGTACAAAAAAGCAGGCTTTAAAGGAACCA    4420
ATTCAGTCGACTGGATCCGGTACC ••• 4444
```

Figure S11: Representative annotated plasmid sequence for cgRNA plasmids in HEK 293T cells. Plasmid: pTrmS-cgQ for cgRNA Q. Numbering begins with the hU6 promoter.

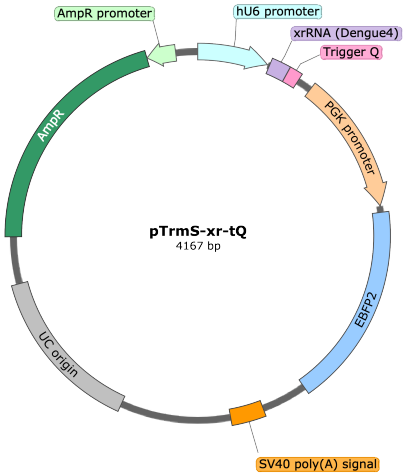

Figure S12: Representative plasmid map for trigger plasmids in HEK 293T cells. Plasmid: pTrmS-xr-tQ for trigger X_Q.

```
...  AAGGTCGGGCAGGAAGAGGGCCTATTTCCCATGATTCCTTCATATTTGCATATACGATACAAGGC    65
     TGTTAGAGAGATAATTAGAATTAATTTGACTGTAAACACAAAGATATTAGTACAAAATACGTGAC   130
     GTAGAAAGTAATAATTTCTTGGGTAGTTTGCAGTTTTAAAATTATGTTTTAAAATGGACTATCAT   195
     ATGCTTACCGTAACTTGAAAGTATTTCGATTTCTTGGCTTTATATATCTTGTGGAAAGGACGAAA   260
     CACCAGTCAGGCCACTTGTGCCACGGTTTGAGCAAACCGTGCTGCCTGTAGCTCCGCCAATAATG   325
     GGAGGCGTAAACATGACAGAAATACGAACGAAACTAACGCGCAAAGATCTTTTTTTCTAGACCCA   390
     GCTTTCTTGTACAAAGTTGGCATTAGACGTCGAGGAATTCTACCGGGTAGGGGAGGCGCTTTTCC   455
     CAAGGCAGTCTGGAGCATGCGCTTTAGCAGCCCCGCTGGGCACTTGGCGCTACACAAGTGGCCTC   520
     TGGCCTCGCACACATTCCACATCCACCGGTAGGCGCCAACCGGCTCCGTTCTTTGGTGGCCCCTT   585
     CGCGCCACCTTCTACTCCTCCCCTAGTCAGGAAGTTCCCCCCCGCCCCGCAGCTCGCGTCGTGCA   650
     GGACGTGACAAATGGAAGTAGCACGTCTCACTAGTCTCGTGCAGATGGACAGCACCGCTGAGCAA   715
     TGGAAGCGGGTAGGCCTTTGGGGCAGCGGCCAATAGCAGCTTTGCTCCTTCGCTTTCTGGGCTCA   780
     GAGGCTGGGAAGGGGTGGGTCCGGGGGCGGGCTCAGGGGCGGGCTCAGGGGCGGGGCGGGCGCCC   845
     GAAGGTCCTCCGGAGGCCCGGCATTCTGCACGCTTCAAAAGCGCACGTCTGCCGCGCTGTTCTCC   910
     TCTTCCTCATCTCCGGGCCTTTCGACCTGCATCCCAAGCTTGCCACCATGGTGAGCAAGGGCGAG   975
     GAGCTGTTCACCGGGGTGGTGCCCATCCTGGTCGAGCTGGACGGCGACGTAAACGGCCACAAGTT  1040
     CAGCGTGAGGGGCGAGGGCGAGGGCGATGCCACCAACGGCAAGCTGACCCTGAAGTTCATCTGCA  1105
     CCACCGGCAAGCTGCCCGTGCCCTGGCCCACCCTCGTGACCACCCTGAGCCACGGCGTGCAGTGC  1170
     TTCGCCCGCTACCCCGACCACATGAAGCAGCACGACTTCTTCAAGTCCGCCATGCCCGAAGGCTA  1235
     CGTCCAGGAGCGCACCATCTTCTTCAAGGACGACGGCAACCTACAAGACCCGCGCCGAGGTGAAGT  1300
     TCGAGGGCGACACCCTAGTGAACCGCATCGAGCTGAAGGGCGTCGACTTCAAGGAGGACGGCAAC  1365
     ATCCTGGGGCACAAGCTGGAGTACAACTTCAACAGCCACAACATCTATATCATGGCCGTCAAGCA  1430
     GAAGAACGGCATCAAGGTGAACTTCAAGATCCGCCACAACGTGGAGGACGGCAGCGTGCAGCTCG  1495
     CCGACCACTACCAGCAGAACACCCCCATCGGCGACGGCCCCGTGCTGCTGCCCGACAGCCACTAC  1560
     CTGAGCACCCAGTCCGTGCTGAGCAAAGACCCCAACGAGAAGCGCGATCACATGGTCCTGCTGGA  1625
     GTTCCGCACCGCCGCCGGGATCACTCTCGGCATGGACGAGCTGTACAAGTAAGTACCACTAGTAC  1690
     CGGTAGATATCAGCCATGGCTTCCCGCCGGCGGTGGCGGCGCAGGATGATGGCACGCTGCCCATG  1755
     TCTTGTGCCCAGGAGAGCGGGATGGACCGTCACCCTGCAGCCTGTGCTTCTGCTAGGATCAATGT  1820
     GTAGGCTAGTCGAGCAGACATGATAAGATACATTGATGAGTTTGGACAAACCACAACTAGAATGC  1885
     AGTGAAAAAAATGCTTTATTTGTGAAATTTGTGATGCTATTGCTTTATTTGTAACCATTATAAGC  1950
     TGCAATAAACAAGTTAACAACAACAATTGCATTCATTTTATGTTTCAGGTTCAGGGGGAGATGTG  2015
     GGAGGTTTTTTAAAGCAAGTAAAACCTCTACAAATGTGGTAAAATCCGATAAGGATCGATCCGGG  2080
     CTGGCGTAATAGCGAAGAGGCCCGCACCGATCGCCCTTCCCAACAGTTGCGCAGCCTGAATGGAT  2145
     GGCCAACGCGCGGGGAGAGGCGGTTTGCGTATTGGGCGCTCTTCCGCTTCCTCGCTCACTGACTC  2210
     GCTGCGCTCGGTCGTTCGGCTGCGGCGAGCGGTATCAGCTCACTCAAAGGCGGTAATACGGTTAT  2275
     CCACAGAATCAGGGGATAACGCAGGAAAGAACATGTGAGCAAAAGGCCAGCAAAAGGCCAGGAAC  2340
     CGTAAAAAGGCCGCGTTGCTGGCGTTTTTCCATAGGCTCCGCCCCCCTGACGAGCATCACAAAAA  2405
     TCGACGCTCAAGTCAGAGGTGGCGAAACCCGACAGGACTATAAAGATACCAGGCGTTTCCCCCTG  2470
     GAAGCTCCCTCGTGCGCTCTCCTGTTCCGACCCTGCCGCTTACCGGATACCTGTCCGCCTTTCTC  2535
     CCTTCGGGAAGCGTGGCGCTTTCTCATAGCTCACGCTGTAGGTATCTCAGTTCGGTGTAGGTCGT  2600
     TCGCTCCAAGCTGGGCTGTGTGCACGAACCCCCCGTTCAGCCCGACCGCTGCGCCTTATCCGGTA  2665
     ACTATCGTCTTGAGTCCAACCCGGTAAGACACGACTTATCGCCACTGGCAGCAGCCACTGGTAAC  2730
     AGGATTAGCAGAGCGAGGTATGTAGGCGGTGCTACAGAGTTCTTGAAGTGGTGGCCTAACTACGG  2795
     CTACACTAGAAGAACAGTATTTGGTATCTGCGCTCTGCTGAAGCCAGTTACCTTCGGAAAAAGAG  2860
     TTGGTAGCTCTTGATCCGGCAAACAAACCACCGCTGGTAGCGGTTTTTTTGTTTGCAAGCAGCAG  2925
     ATTACGCGCAGAAAAAAAGGATCTCAAGAAGATCCTTTGATCTTTTCTACGGGGTCTGACGCTCA  2990
     GTGGAACGAAAACTCACGTTAAGGGATTTTGGTCATGAGATTATCAAAAAGGATCTTCACCTAGA  3055
     TCCTTTTAAATTAAAAATGAAGTTTTAAATCAATCTAAAGTATATATGAGTAAACTTGGTCTGAC  3120
     AGTTACCAATGCTTAATCAGTGAGGCACCTATCTCAGCGATCTGTCTATTTCGTTCATCCATAGT  3185
     TGCCTGACTCCCCGTCGTGTAGATAACTACGATACGGGAGGGCTTACCATCTGGCCCCAGTGCTG  3250
     CAATGATACCGCGCGACCCACGCTCACCGGCTCCAGATTTATCAGCAATAAACCAGCCAGCCGGA  3315
     AGGGCCGAGCGCAGAAGTGGTCCTGCAACTTTATCCGCCTCCATCCAGTCTATTAATTGTTGCCG  3380
     GGAAGCTAGAGTAAGTAGTTCGCCAGTTAATAGTTTGCGCAACGTTGTTGCCATTGCTACAGGCA  3445
     TCGTGGTGTCACGCTCGTCGTTTGGTATGGCTTCATTCAGCTCCGGTTCCCAACGATCAAGGCGA  3510
     GTTACATGATCCCCCATGTTGTGCAAAAAAGCGGTTAGCTCCTTCGGTCCTCCGATCGTTGTCAG  3575
     AAGTAAGTTGGCCGCAGTGTTATCACTCATGGTTATGGCAGCACTGCATAATTCTCTTACTGTCA  3640
     TGCCATCCGTAAGATGCTTTTCTGTGACTGGTGAGTACTCAACCAAGTCATTCTGAGAATAGTGT  3705
     ATGCGGCGACCGAGTTGCTCTTGCCCGGCGTCAATACGGGATAATACCGCGCCACATAGCAGAAC  3770
     TTTAAAAGTGCTCATCATTGGAAAACGTTCTTCGGGGCGAAAACTCTCAAGGATCTTACCGCTGT  3835
     TGAGATCCAGTTCGATGTAACCCACTCGTGCACCCAACTGATCTTCAGCATCTTTTACTTTCACC  3900
     AGCGTTTCTGGGTGAGCAAAAACAGGAAGGCAAAATGCCGCAAAAAAGGGAATAAGGGCGACACG  3965
     GAAATGTTGAATACTCATACTCTTCCTTTTTCAATATTATTGAAGCATTTATCAGGGTTATTGTC  4030
     TCATGAGCGGATACATATTTGAATGTATTTAGAAAAATAAACAAATAGGGGTTCCGCGCACATTT  4095
     CCCCGAAAAGTGCCACCTTGTACAAAAAAGCAGGCTTTAAAGGAACCAATTCAGTCGACTGGATC  4160
     CGGTACC ...  4167
```

Figure S13: Representative annotated plasmid sequence for trigger plasmids in HEK 293T cells. Plasmid: pTrmS-xr-tQ for trigger X_Q. Numbering begins with the hU6 promoter.

S4 Schematics of putative ON and OFF states

S4.1 Constitutively active terminator switch cgRNA (ON→OFF logic)

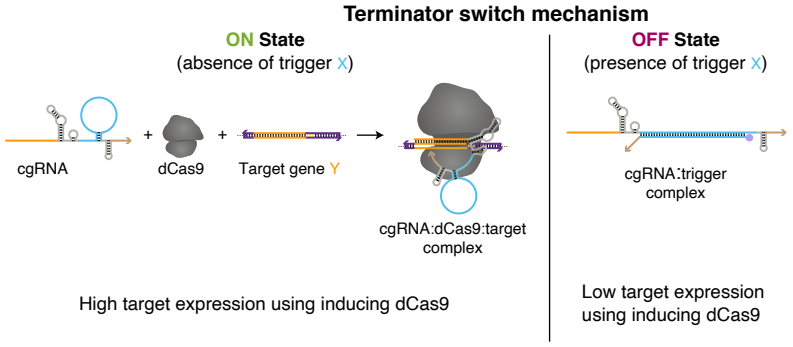

Figure S14: Schematics of putative ON and OFF states for the terminator switch mechanism. ON state: the terminator switch cgRNA is constitutively active, directing the function of protein effector dCas9 to a target gene Y in the absence of trigger; the extended loop and modified sequence domains in the terminator region (blue) are intended not to interfere with the activity of the cgRNA:dCas9 complex. OFF state: in the presence of RNA trigger X, hybridization of the trigger is intended to form a structure incompatible with cgRNA mediation of dCas9 function.

S4.2 Constitutively inactive split-terminator switch cgRNA (OFF→ON logic)

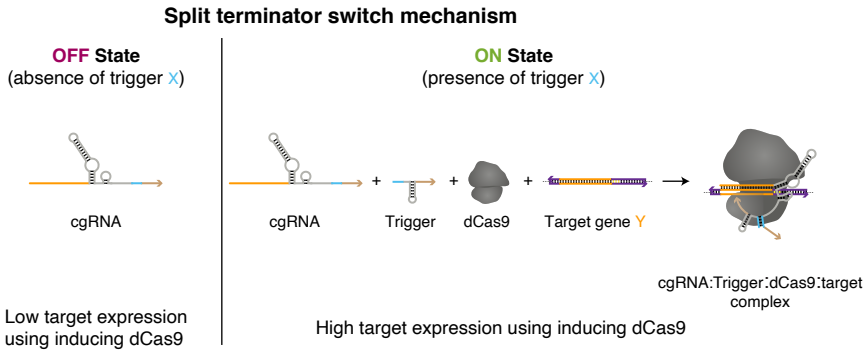

Figure S15: Schematics of putative OFF and ON states for the split-terminator switch mechanism. OFF state: the split-terminator switch cgRNA is constitutively inactive. In the absence of RNA trigger X, the cgRNA is incapable of directing the function of the protein effector dCas9. ON state: the complex of cgRNA and trigger X with protein effector dCas9 induces target gene Y. The modified sequence domains in the terminator duplex (blue) are intended not to interfere with the activity of the cgRNA:trigger:dCas9 complex.

S5 Flow cytometry replicates in HEK 293 T cells

Flow cytometry replicates are shown for conditional response and crosstalk studies in Section S5.1 for the terminator switch cgRNAs of Figure 4 and in Section S5.2 for split-terminator switch cgRNAs of Figure 5. In Section S5.3, these replicates are used to quantify the ON state, OFF state, fold change (ON:OFF ratio), dynamic range, and fractional dynamic range of each cognate cgRNA/trigger pair. In Section S5.4, the crosstalk between non-cognate cgRNA/trigger pairs is quantified using uncertainty propagation as detailed in Section S1.4.

S5.1 Constitutively active terminator switch

S5.1.1 ON state, OFF state, and conditional response (cf. Figure 4)

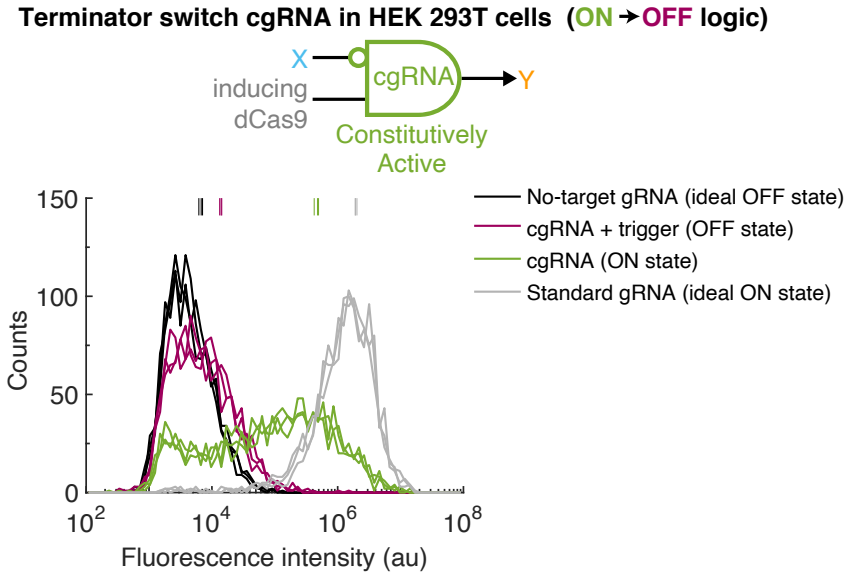

Figure S16: Flow cytometry replicates for terminator switch ON state, OFF state, and conditional response in HEK 293T cells (cf. Figure 4). (a) Single-cell fluorescence intensities. Expression of RNA trigger X toggles the cgRNA from ON→OFF, leading to a decrease in fluorescence. Transient expression of inducing dCas9 and PhiYFP target gene Y and either: standard gRNA + no-trigger control (ideal ON state), cgRNA + no-trigger control (ON state), cgRNA + RNA trigger X (OFF state), no-target gRNA that lacks target-binding region + no-trigger control (ideal OFF state). Traces of the same color correspond to $N = 3$ replicate wells transfected on the same day and assayed via flow cytometry after 24 h ($M = 1200$ cells from the high-transfection gate per well). The mean for each replicate is displayed as a vertical line.

S5.1.2 Orthogonal library studies (cf. Figure 4)

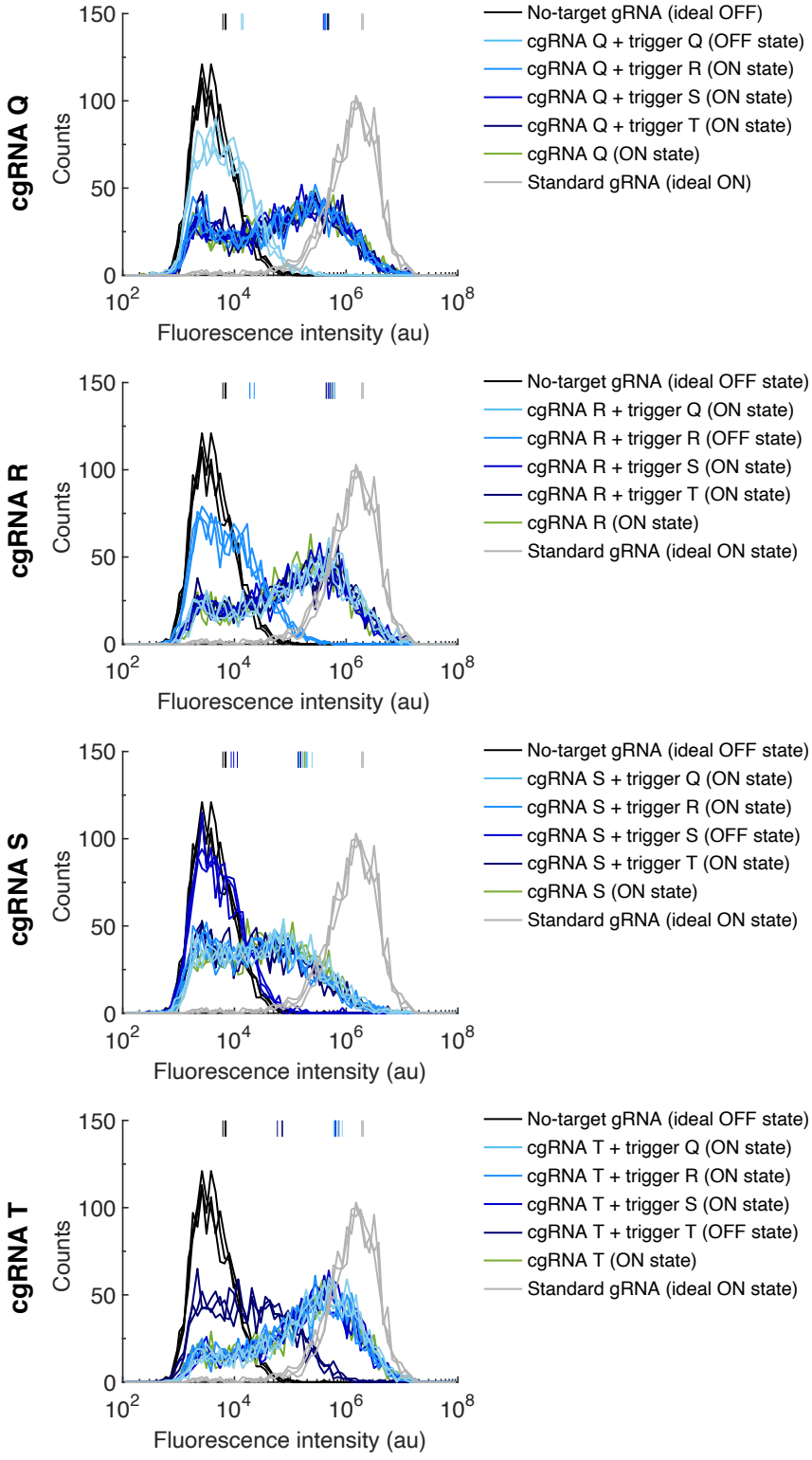

Figure S17: Flow cytometry replicates for terminator switch orthogonal response in HEK 293T cells (cf. Figure 4). (a) Single-cell fluorescence intensities for cgRNAs Q, R, S, T. Transient expression of inducing dCas9 and PhiYFP target gene Y and either: standard gRNA + no-trigger control (Ideal ON state), cgRNA + no-trigger control (ON state), cgRNA + cognate trigger (OFF state), cgRNA + a non-cognate trigger (ON state), or no-target gRNA that lacks target-binding region + no-trigger control (ideal OFF state). Expression of the cognate RNA trigger (X_Q for cgRNA Q, X_R for cgRNA R, X_S for cgRNA S, X_T for cgRNA T) toggles the cgRNA from ON→OFF, leading to a decrease in fluorescence. Traces of the same color correspond to $N = 3$ replicate wells transfected on the same day and assayed via flow cytometry after 24 h ($M = 1200$ cells from the high-transfection gate per well). The mean for each replicate is displayed as a vertical line.

S5.2 Constitutively inactive split-terminator switch

S5.2.1 ON state, OFF state, and conditional response (cf. Figure 5)

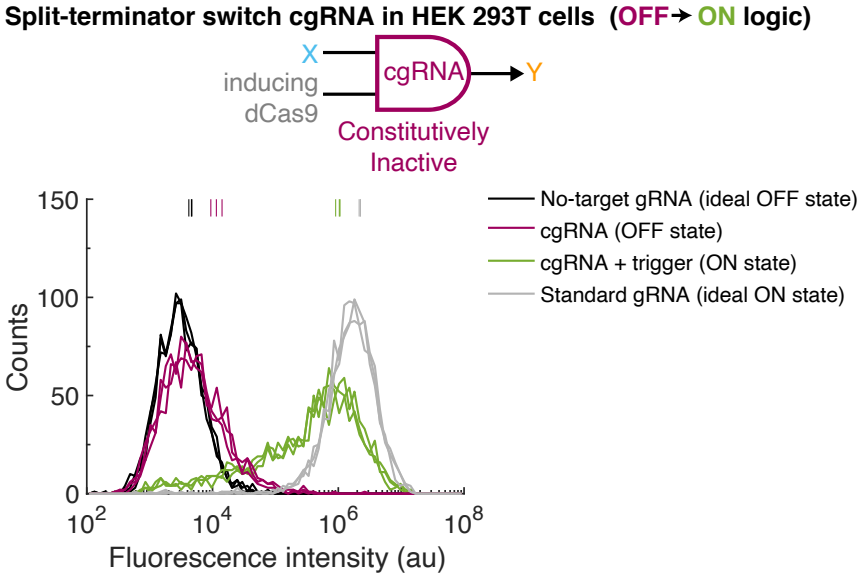

Figure S18: Flow cytometry replicates for split-terminator switch ON state, OFF state, and conditional response in HEK 293T cells (cf. Figure 5). (a) Single-cell fluorescence intensities. Expression of RNA trigger X toggles the cgRNA from OFF→ON, leading to an increase in fluorescence. Transient expression of inducing dCas9 and PhiYFP target gene Y and either: no-target gRNA that lacks target-binding region + no-trigger control (ideal OFF state), cgRNA + no-trigger control (OFF state), cgRNA + RNA trigger X (ON state), standard gRNA + no-trigger control (ideal ON state). Traces of the same color correspond to $N = 3$ replicate wells transfected on the same day and assayed via flow cytometry after 24 h (M=1000 cells from the high-transfection gate per well). The mean for each replicate is displayed as a vertical line.

S5.2.2 Orthogonal library studies (cf. Figure 5)

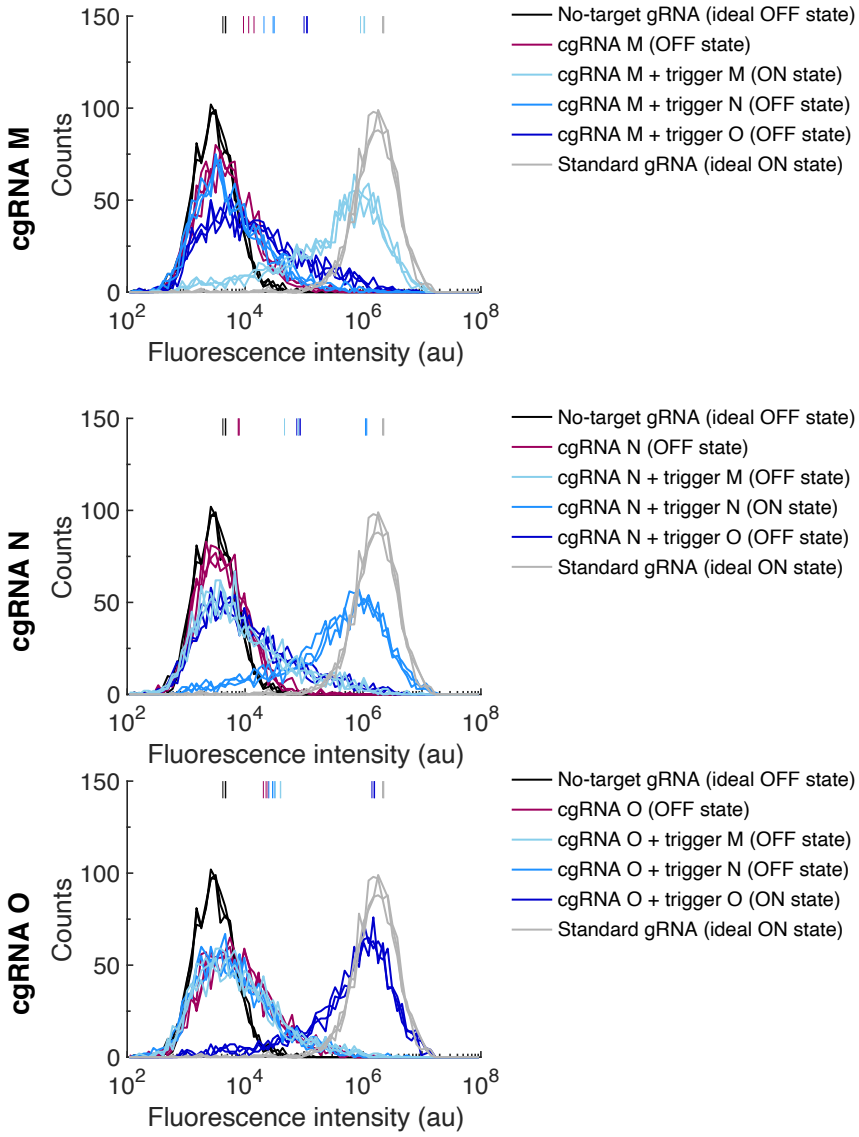

Figure S19: Flow cytometry replicates for split-terminator switch orthogonal response in HEK 293T cells (cf. Figure 5). (a) Single-cell fluorescence intensities for cgRNAs M, N, O. Transient expression of inducing dCas9 and PhiYFP target gene Y and either: no-target gRNA that lacks target-binding region + no-trigger control (ideal OFF state), cgRNA + no-trigger control (OFF state), cgRNA + a non-cognate trigger (OFF state), cgRNA + cognate trigger (ON state), standard gRNA + no-trigger control (ideal ON state). Expression of the cognate RNA trigger X (X_M for cgRNA M, X_N for cgRNA N, X_O for cgRNA O) toggles the cgRNA from OFF→ON, leading to an increase in fluorescence. Traces of the same color correspond to $N = 3$ replicate wells transfected on the same day and assayed via flow cytometry after 24 h. (M=1000 cells from the high-transfection gate per well). The mean for each replicate is displayed as a vertical line.

S5.3 Quantifying ON state, OFF state, fold change, dynamic range, and fractional dynamic range

	cgRNA	ON	OFF	Fold Change (ON:OFF)	Dynamic Range (DR)	Fractional Dynamic Range (FDR)
a	**Terminator switch mechanism (ON→OFF logic) in HEK 293T cells**					
	Ideal	$1\,950\,000 \pm 40\,000$	0 ± 300		$1\,950\,000 \pm 40\,000$	1.00 ± 0.03
	cgRNA Q	$440\,000 \pm 20\,000$	6300 ± 400	70 ± 6	$440\,000 \pm 20\,000$	0.22 ± 0.01
	cgRNA R	$480\,000 \pm 20\,000$	$12\,900 \pm 1300$	37 ± 4	$470\,000 \pm 20\,000$	0.24 ± 0.01
	cgRNA S	$170\,000 \pm 6000$	2000 ± 600	90 ± 30	$168\,000 \pm 6000$	0.086 ± 0.003
	cgRNA T	$680\,000 \pm 20\,000$	$58\,000 \pm 4000$	11.7 ± 0.9	$630\,000 \pm 30\,000$	0.321 ± 0.014
b	**Split-terminator switch mechanism (OFF→ON logic) in HEK 293T cells**					
	Ideal	$2\,190\,000 \pm 30\,000$	0 ± 140		$2\,190\,000 \pm 30\,000$	1.00 ± 0.02
	cgRNA M	$1\,020\,000 \pm 30\,000$	7000 ± 1000	150 ± 20	$1\,010\,000 \pm 30\,000$	0.46 ± 0.02
	cgRNA N	$1\,090\,000 \pm 30\,000$	3000 ± 200	360 ± 30	$1\,090\,000 \pm 30\,000$	0.498 ± 0.014
	cgRNA O	$1\,510\,000 \pm 40\,000$	$18\,900 \pm 400$	80 ± 3	$1\,490\,000 \pm 40\,000$	0.68 ± 0.02

Table S14: Quantifying ON state, OFF state, fold change, dynamic range, and fractional dynamic range (cf. Figures 4 and 5). (a) Terminator switch in HEK 293T cells (cf. Figure 4). (b) Split-terminator switch in HEK 293T cells (cf. Figure 5). See Section S1.4 for detailed definitions of ON state, OFF state, fold change, ideal ON state, ideal OFF state, dynamic range, and fractional dynamic range. ON and OFF values are background-subtracted mean fluorescent signal. For the terminator switch (ON→OFF logic): ON = (cgRNA + no-trigger control using random pool) − (no-target gRNA + no-trigger control using random pool); OFF = (cgRNA + cognate trigger) − (no-target gRNA + cognate trigger). For split-terminator switch (OFF→ON logic): OFF = (cgRNA + no-trigger control using random pool) − (no-target gRNA + no-trigger control using random pool); ON = (cgRNA + cognate trigger) − (no-target gRNA + cognate trigger). For both mechanisms: ideal ON = (standard gRNA + no-trigger control using random pool) - (no-target gRNA + no-trigger control using random pool); ideal OFF = (no-target gRNA + no-trigger control using random pool) - (no-target gRNA + no-trigger control using random pool); fold change = ON/OFF, dynamic range = ON − OFF, fractional dynamic range = [ON−OFF]/[ideal ON − ideal OFF]. Mean ± estimated standard error of the mean (with uncertainty propagation) based on the mean single-cell fluorescence over 1545–3970 cells (terminator switch) or 1017–2394 cells (split-terminator switch) for each of $N = 3$ replicate wells.

S5.4 Quantifying crosstalk for non-cognate cgRNA/trigger pairs

	cgRNA	Trigger	Signal (SIG)		Crosstalk (CT)	
a	**Terminator switch mechanism (ON→OFF logic) in HEK 293T cells**					
	Q	no-trigger control	440 000	± 20 000		
	Q	X_Q	6300	± 400	1.00	± 0.06
	Q	X_R	400 000	± 10 000	0.09	± 0.05
	Q	X_S	420 000	± 20 000	0.06	± 0.06
	Q	X_T	430 000	± 20 000	0.02	± 0.06
	R	no-trigger control	480 000	± 20 000		
	R	X_Q	566 000	± 13 000	−0.18	± 0.05
	R	X_R	12 900	± 1300	1.00	± 0.05
	R	X_S	460 000	± 20 000	0.05	± 0.05
	R	X_T	560 000	± 20 000	−0.16	± 0.06
	S	no-trigger control	170 000	± 6000		
	S	X_Q	192 000	± 13 000	−0.13	± 0.08
	S	X_R	150 000	± 10 000	0.09	± 0.08
	S	X_S	2000	± 600	1.00	± 0.05
	S	X_T	150 000	± 4000	0.12	± 0.04
	T	no-trigger control	680 000	± 20 000		
	T	X_Q	780 000	± 30 000	−0.15	± 0.06
	T	X_R	640 000	± 30 000	0.07	± 0.06
	T	X_S	680 000	± 30 000	0.00	± 0.06
	T	X_T	58 000	± 4000	1.00	± 0.06
b	**Split-terminator switch mechanism (OFF→ON logic) in HEK 293T cells**					
	M	no-trigger control	7000	± 1000		
	M	X_M	1 020 000	± 30 000	1.00	± 0.05
	M	X_N	24 000	± 3000	0.016	± 0.004
	M	X_O	110 000	± 4000	0.102	± 0.005
	N	no-trigger control	30 000	± 200		
	N	X_M	67 000	± 7000	0.059	± 0.007
	N	X_N	1 090 000	± 30 000	1.00	± 0.03
	N	X_O	74 000	± 3000	0.065	± 0.003
	O	no-trigger control	18 900	± 400		
	O	X_M	34 000	± 3000	0.010	± 0.002
	O	X_N	23 000	± 2000	0.003	± 0.001
	O	X_O	1 510 000	± 40 000	1.00	± 0.04

Table S15: Quantifying crosstalk for cognate and non-cognate cgRNA/trigger pairs. (a) Terminator switch in HEK 293T cells (cf. Figure 4). (b) Split-terminator switch in HEK 293T cells (cf. Figure 5). See Section S1.4 for detailed definitions of signal and crosstalk. Mean ± estimated standard error of the mean (with uncertainty propagation) based on the mean single-cell fluorescence over 1545–3970 cells (terminator switch) or 1017–2394 cells (split-terminator switch) for each of $N = 3$ replicate wells.

S6 Additional Studies in HEK 293T Cells

S6.1 Testing the FE-modified Cas9 handle for terminator switch cgRNAs

The "flip+extend" (FE) modification to the Cas9 handle has been shown to improve gRNA performance,[9] combining flipping an A-U base pair to remove a putative Pol(III) termination site caused by UUUU in the Cas9 handle sequence and extending the Cas9 handle by 5 bp. The terminator switch cgRNAs characterized in Figure 4 use the standard Cas9 handle. We wondered whether using the FE modification would increase the fractional dynamic range of our cgRNAs by increasing the strength of the ON state. Indeed, this turned out to be the case, but we also observed a less clean OFF state (Figure S20d). As a result, for our library of 4 orthogonal cgRNAs using the FE modification, the median fold-change decreased from $\approx$50$\times$ (Figure 4e) to $\approx$25$\times$ (Figure S20e), but the median fractional dynamic range increased from $\approx$20% (Figure 4a) to $\approx$50% (Figure S20a). Depending on the application, one might prioritize fold change (cgRNAs without FE modification) or fractional dynamic range (cgRNAs with FE modification).

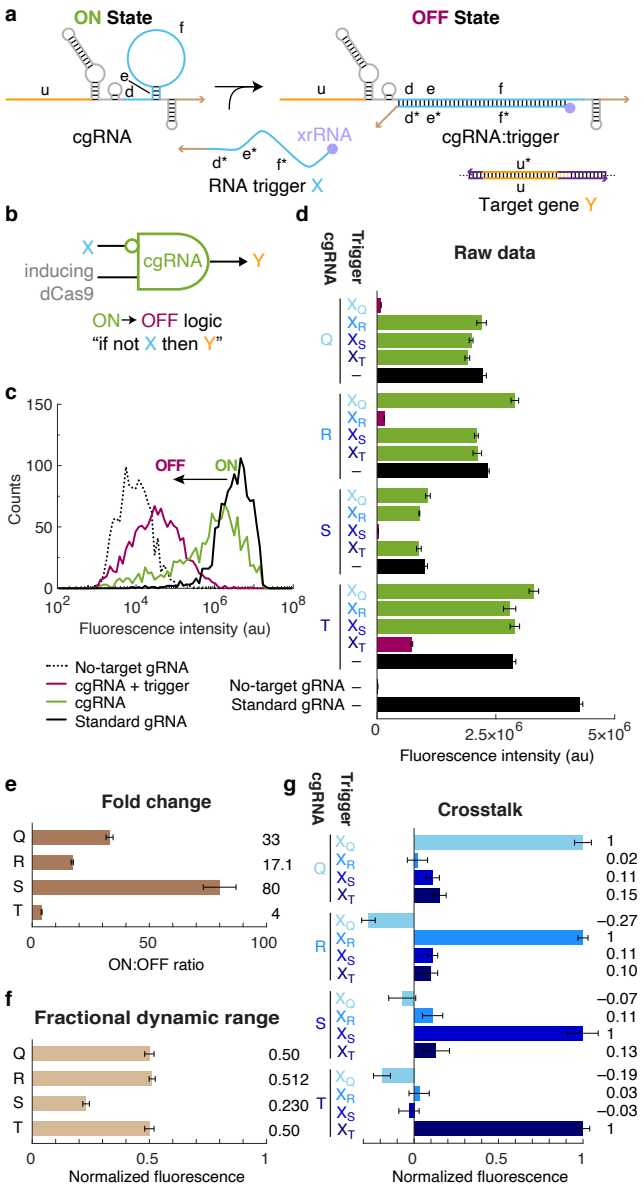

Figure S20: Testing the FE-modified Cas9 handle for allosteric ON→OFF terminator switch cgRNAs with inducing dCas9 in HEK 293T cells (cf. Figure 4). (a) cgRNA mechanism: the constitutively active cgRNA is inactivated by hybridization of RNA trigger X. Rational design of cgRNA terminator region (domains "d-e-f": 6 nt linker, 4 nt stem, 30 nt loop) and complementary trigger region (domains "f*-e*-d*"). (b) Conditional logic: "if not X then Y". (c) Expression of RNA trigger X (xrRNA + 40 nt unstructured + hU6 terminator) toggles the cgRNA from ON→OFF, leading to a decrease in fluorescence. Single-cell fluorescence intensities via flow cytometry. Transfection of plasmids expressing inducing dCas9-VPR, Phi-YFP target gene Y, and either: standard gRNA + no-trigger control (ideal ON state), cgRNA + no-trigger control (ON state), cgRNA + RNA trigger X (OFF state), no-target gRNA that lacks target-binding region + no-trigger control (ideal OFF state). (d-g) Programmable conditional regulation using 4 orthogonal cgRNAs (Q, R, S, T). (d) Raw fluorescence depicting ON→OFF conditional response to cognate trigger. (e) Fold change = ON/OFF. (f) Fractional dynamic range = (ON − OFF)/(ideal ON − ideal OFF). (g) Crosstalk = (ON − SIG_p)/(ON − OFF) where SIG_p corresponds to signal for cgRNA + trigger p for $p \in \{\mathrm{X_Q}, \mathrm{X_R}, \mathrm{X_S}, \mathrm{X_T}\}$. Bar graphs depict mean ± estimated standard error of the mean (with uncertainty propagation) calculated based on the mean single-cell fluorescence over 1240–4516 cells for each of $N = 3$ replicate wells.

S6.2 Testing terminator switch trigger X_Q with different 5′ xrRNA variants

xrRNAs protect viral RNAs from degradation,[18,19] but to our knowledge, have not been previously used in a synthetic biology setting. As a result, we decided to test a variety of xrRNA motifs from 5 different flaviviruses in search of xrRNA structure/sequence combinations suitable for enhancing the performance of short RNA triggers. Murray Valley encephalitus, West Nile virus, and Zika contain tandem xrRNA pseudoknot motifs each with an adjacent hairpin while Dengue and Yellow fever contain one xrRNA pseudoknot motif with an adjacent hairpin.[1] We tested 12 variants as described in Table S16; the sequences are provided in Table S7. Using terminator switch cgRNA Q as a test case, Figure S21 compares the OFF state using a standard trigger vs a trigger with a 5′ xrRNA variant. A wide range of effects is observed, with some xrRNAs dramatically improving trigger performance (e.g., xr6 and xr11), others dramatically hindering trigger performance (e.g., xr3 and xr4), and one having little effect on trigger performance (xr12). The best performing variants (xr2, xr6, and xr11) all consisted of the first xrRNA pseudoknot motif with adjacent hairpin. Based on these results, we selected variant xr11 (Dengue 4) to append to the 5′ end of all trigger sequences for terminator switch cgRNA studies (e.g., Figure 4).

Variant	Virus	Description
xr1	MVE	first xrRNA pseudoknot
xr2	MVE	first xrRNA pseudoknot + adjacent hairpin
xr3	MVE	spacer + first xrRNA pseudoknot + adjacent hairpin
xr4	MVE	spacer + first xrRNA pseudoknot + adjacent hairpin + second xrRNA pseudoknot + adjacent hairpin
xr5	WNV	first xrRNA pseudoknot
xr6	WNV	first xrRNA pseudoknot + adjacent hairpin
xr7	WNV	first xrRNA pseudoknot + adjacent hairpin + second xrRNA pseudoknot + adjacent hairpin
xr8	Zika	first xrRNA pseudoknot
xr9	Zika	first xrRNA pseudoknot + adjacent hairpin
xr10	Zika	first xrRNA pseudoknot + adjacent hairpin + second xrRNA pseudoknot + adjacent hairpin
xr11	Dengue	sole xrRNA pseudoknot + adjacent hairpin
xr12	YF	sole xrRNA pseudoknot + adjacent hairpin

Table S16: Description of tested xrRNA variants taken from 5 flaviviruses: Murray Valley encephalitis (MVE, NC_000943.1),[1,2] West Nile virus (WNV, NC_001563.2),[1] Zika (NC_012532.1),[1] Dengue (Dengue 4, NC_002640.1),[1] Yellow fever (YF, NC_002031.1).[1]

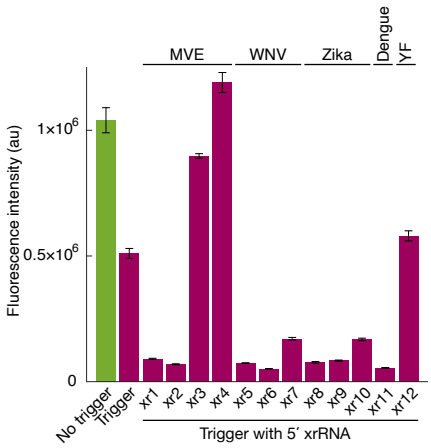

Figure S21: Testing terminator switch trigger X_Q with different 5′ xrRNA variants in HEK 293T cells. All samples include the terminator switch cgRNA Q. The no-trigger control uses a random pool of triggers to provide a sequence-generic approximation of the metabolic load of trigger expression. All of the remaining samples use terminator switch trigger X_Q with the noted xrRNA variant appended 5′ of the trigger. xrRNA variants are described in Table S16 and sequences are provided in Table S7. Bar graphs depict mean ± estimated standard error of the mean calculated based on the mean single-cell fluorescence over 487–3906 cells for each of $N = 3$ replicate wells.

S6.3 Testing a Dengue xrRNA at different locations on a standard gRNA, the terminator switch cgRNA Q, and trigger X_Q

After observing that appending variant xr11 (Dengue4) to the 5′ end of trigger X_Q significantly improves trigger function (leading to a cleaner OFF state; Figure S21), we wondered whether we could likewise enhance the function of a standard gRNA by appending a 5′ xrRNA. In fact, we observed the opposite, with xr11 significantly decreasing the function of a standard gRNA (Figure S22a; compare bars 1 and 2). This degradation in gRNA performance was observed whether or not a 20-nt spacer was included between the xrRNA and the gRNA (compare bars 2 and 3) to reduce the potential for steric inhibition of gRNA:Cas function. Appending xr11 to the 5′ end of cgRNA Q leads to an even more extreme degradation of cgRNA function, eliminating the ON state completely (compare bars 4 and 5). These results are not entirely surprising because our preliminary studies have typically revealed a decrease in gRNA/cgRNA function when additional sequence is appended to the 5′ end. gRNAs/cgRNAs may also benefit from some protection against degradation when bound to Cas9, potentially reducing the motivation for additional protection.

In nature, xrRNAs are thought to protect flaviviruses from degradation by forming a mechanical block against 5′ exoribonucleases.[20] Consistent with this observation, xr11 dramatically improves trigger function when appended 5′ of the trigger (Figure S22b; compare bars 9 and 11). However, we were curious whether placing the xrRNA 3′ of the trigger would have any effect. In fact, it did not (with the xrRNA in either the forward or the reverse direction; compare bars 13 and 14 to bar 9).

For the beneficial case where xr11 is appended 5′ of the trigger, we further found that it made no observable difference if we included a G ahead of the xrRNA (compare lanes 11 and 12) as a potential means of enhancing the strength of the transcription start site.[17]

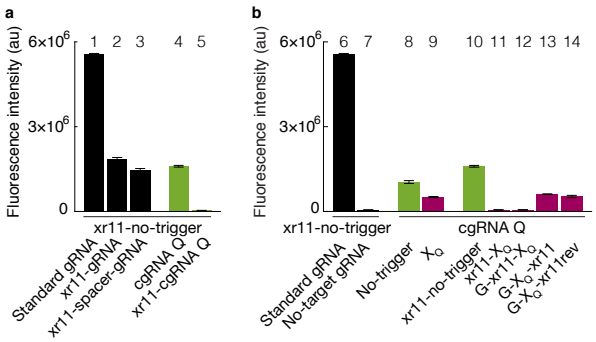

Figure S22: Testing a Dengue xrRNA at different locations on a standard gRNA, the terminator switch cgRNA Q, and trigger X_Q in HEK 293T cells. (a) xrRNA modifications to a standard gRNA and cgRNA Q. (b) xrRNA modifications to trigger X_Q. The "no-trigger" and "xr11-no-trigger" controls using a random pool of triggers (without or with xr11 appended to the 5′ end) to provide a sequence-generic approximation of the metabolic load of trigger expression. The trigger names beginning with "G" include a G at the 5′ end as a potential enhancer of the strength of the transcription start site.[17] Sequences are provided in Tables S4, S5, S8, and S9. Bar graphs depict mean ± estimated standard error of the mean calculated based on the mean single-cell fluorescence over 487–3906 cells for each of $N = 3$ replicate wells.

S6.4 Comparison of terminator switch performance using triggers with and without a 5′ Dengue xrRNA

Figures S23 and S24a demonstrates the substantial improvement in conditional response for a library of four terminator switch cgRNAs (Q, R, S, T; ON→OFF logic) using cognate triggers with a 5′ xrRNA (Dengue 4, NC_002640.1).[1] The cleaner OFF state using triggers with a 5′ xrRNA leads to a dramatic increase in fold change (Figure S24b), and a noticeable increase in fractional dynamic range (Figure S24c).

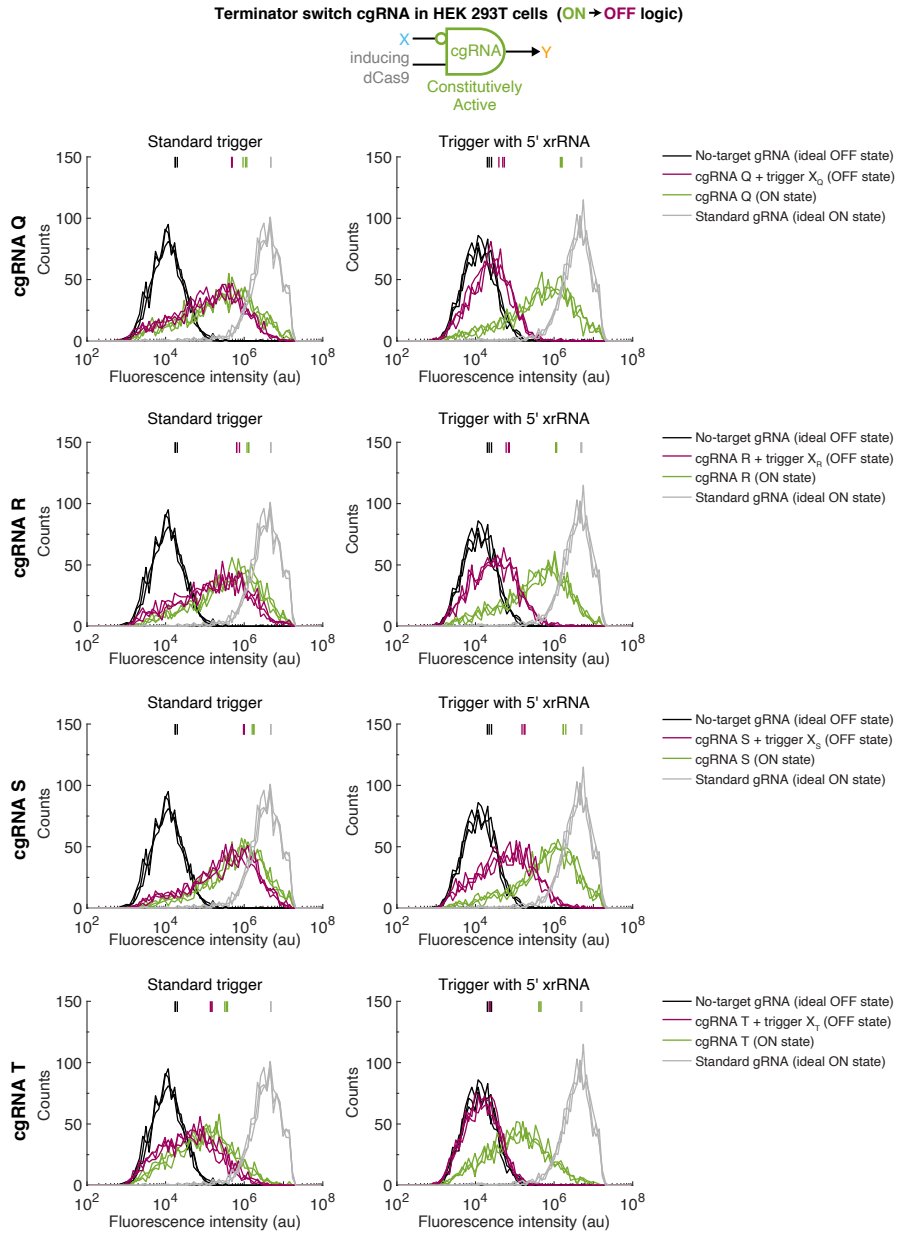

Figure S23: Flow cytometry replicates for terminator switch performance using triggers with and without a 5′ Dengue xrRNA in HEK 293T cells (cf. Figure 3c). (a) Single-cell fluorescence intensities. Expression of RNA trigger X toggles the cgRNA from ON→OFF, leading to a decrease in fluorescence. Transient expression of inducing dCas9 and PhiYFP target gene Y and either: standard gRNA + no-trigger control (ideal ON state), a cgRNA + no-trigger control (Q, R, S, or T; ON state), cgRNA + cognate RNA trigger (X_Q for cgRNA Q, X_R for cgRNA R, X_S for cgRNA S, X_T for cgRNA T; OFF state), no-target gRNA that lacks target-binding region + no-trigger control (ideal OFF state). Traces of the same color correspond to $N = 3$ replicate wells transfected on the same day and assayed via flow cytometry after 24 h ($M = 1000$ cells from the high-transfection gate per well). The mean for each replicate is displayed as a vertical line.

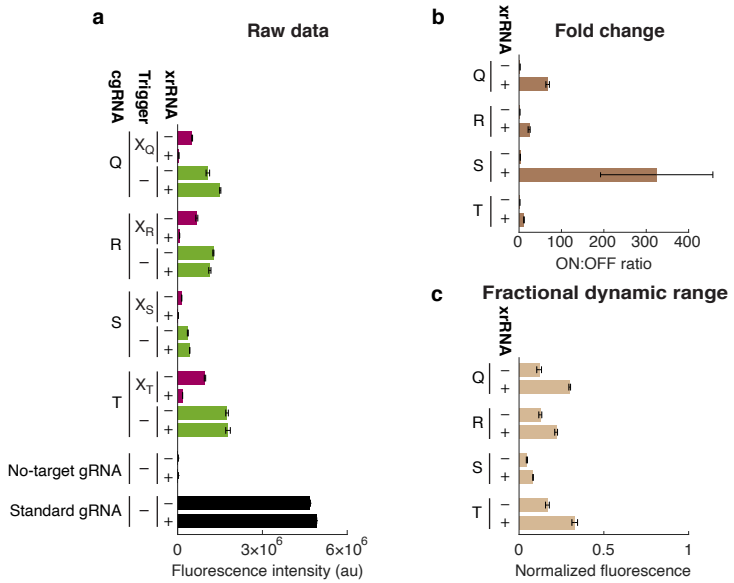

Figure S24: Comparison of terminator switch performance using triggers with and without a 5′ Dengue xrRNA in HEK 293T cells (cf. Figure 3c). Expression of RNA trigger X (±xrRNA + 40 nt unstructured + hU6 terminator) toggles the cgRNA from ON→OFF, leading to a decrease in fluorescence. Transfection of plasmids expressing inducing dCas9-VPR, Phi-YFP target gene Y, and either: standard gRNA + no-trigger control (ideal ON state), cgRNA + no-trigger control (ON state), cgRNA + RNA trigger X (OFF state), no-target gRNA that lacks target-binding region + no-trigger control (ideal OFF state). Programmable conditional regulation using 4 orthogonal cgRNAs (Q, R, S, T). Sequences are provided in Tables S4 and S5. (a) Raw fluorescence depicting ON→OFF conditional response to cognate trigger. (b) Fold change = ON/OFF. (c) Fractional dynamic range = (ON − OFF)/(ideal ON − ideal OFF). Bar graphs depict mean ± estimated standard error of the mean (with uncertainty propagation) calculated based on the mean single-cell fluorescence over 1067–4358 cells for each of $N = 3$ replicate wells.

S6.5 Truncating a standard gRNA to identify candidate split sites for the split-terminator switch mechanism

As a starting point for devising the split-terminator switch mechanism, we set out to measure how many nucleotides needed to be removed from the 3′-end of a standard gRNA to eliminate function. The goal was to find a truncation location that yielded a clean OFF state (no gRNA function). We investigated truncations at four locations (Figure S25): 3′ of the Cas9 handle (45 nt deletion), 3′ of the nexus hairpin (32 nt deletion), in the loop of terminator hairpin 1 (23 nt deletion), and in the loop of terminator hairpin 2 (8 nt deletion). The results of Figure S26 reveal that deleting as few as 8 nt from the 3′ end of the gRNA severely impairs function (corresponding to diminished induction of PhiYFP). For the remaining truncated gRNAs (45 nt, 32 nt, and 23 nt deletions), PhiYFP fluorescence is equivalent to the no-target gRNA control (ideal OFF state).

Our terminator switch mechanism for ON→OFF logic (Figure 4a) previously demonstrated that the stem of terminator hairpin 1 is designable.[8] This knowledge suggested eliminating the loop of terminator hairpin 1 to create an allosteric split-terminator switch cgRNA (OFF→ ON logic) with the cgRNA corresponding to the 5′ fragment containing the target binding sequence and the Cas9 handle, and the trigger corresponding to the 3′ fragment. In that scenario: 1) the results of Figure S26 indicated that the cgRNA would have a clean OFF state with total loss of function in the absence of the trigger, 2) the likely designability of the new "terminator duplex" formed by hybridization of the trigger to the cgRNA suggested an avenue for designing allosteric cgRNAs with trigger X independent of regulatory target Y (in addition to designability of libraries of orthogonal cgRNA/trigger pairs). The question remained as to whether the cgRNA:trigger complex would be functional with a terminator duplex replacing the original terminator hairpin 1, and further, what length the terminator duplex should be to optimize performance (see Section S6.6).

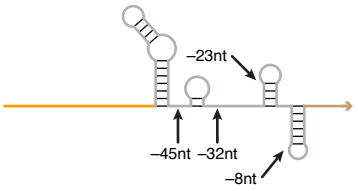

Figure S25: Truncating a standard gRNA to identify candidate split sites for the split-terminator switch mechanism. The 3′ portion of the gRNA was truncated at each of four locations (corresponding to deletion of 45 nt, 32 nt, 23 nt, or 8 nt) and then the remaining 5′ gRNA fragment was tested for function in HEK 293T cells. Arrows indicate approximate truncation locations in the gRNA structure. Refer to Table S10 for sequences.

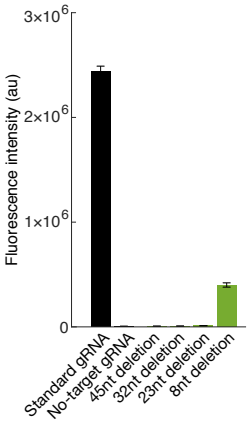

Figure S26: Testing truncations of a standard gRNA to identify candidate split sites for the split-terminator switch mechanism in HEK 293T cells. To create truncated gRNAs, nucleotides were deleted from the 3′ end of a standard gRNA; see Figure S25 for truncation locations and Table S10 for sequences. Transfection of plasmids expressing inducing dCas9-VPR, Phi-YFP target gene Y, and either: standard gRNA + no-trigger control (ideal ON state), no-target gRNA that lacks target-binding region + no-trigger control (ideal OFF state), the 5′ portion of a truncated gRNA + no-trigger control. Bar graphs depict mean ± estimated standard error of the mean calculated based on the mean single-cell fluorescence over 2114–3085 cells for each of $N = 3$ replicate wells.

S6.6 Optimizing the length of terminator duplex for the split-terminator switch mechanism

We set out to test whether the split-terminator switch cgRNA mechanism would be functional with a terminator duplex (formed via hybridization between the cgRNA and the trigger) replacing terminator hairpin 1 (see Section S6.5). Furthermore, we wanted to determine what length of terminator duplex would optimize the strength of the ON state. The terminator duplex is formed via hybridization between domain 'd' of the cgRNA and the reverse complementary domain 'd*' in the trigger. For our first exploratory study, we designed a split-terminator switch with |d| = 40 nt and then truncated the terminator duplex to obtain designs with |d| = 30 nt, 20 nt, and 10 nt. We were surprised to find that not only were all of these variants functional (Figure S27), the strongest ON state was achieved with |d| = 10 nt, which we had expected to be too short for stable hybridization in a cellular setting. To further validate this domain dimension, we designed and tested a library of three orthogonal cgRNA/trigger pairs with |d| = 10 nt that performed very well (Figure S28; median fold change $\approx 40\times$, median fractional dynamic range $\approx$ 40%, median crosstalk $\approx$ 9%). We then decided to shorten the terminator duplex even further in an effort to identify the minimum terminator duplex length. To do this, we took the library of three orthogonal cgRNA/trigger pairs with |d| = 10 nt and truncated the terminator duplex of each to obtain designs with |d| = 8 nt, 6 nt, and 4 nt. To our even greater surprise, the shortest terminator duplex with |d| = 4 nt performed very well with a strong ON state and a clean OFF state (Figure S29). On the one hand, this might seem unsurprising considering that the original terminator hairpin 1 has a stem with 4 base pairs. On the other hand, the fact that the 4 bp terminator duplex forms in a cellular environment is unexpected and suggests that the terminator duplex is stabilized by binding of the cgRNA and trigger with Cas9. Additional study is warranted.

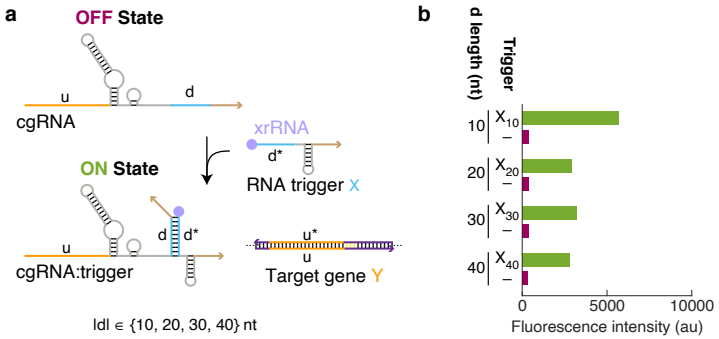

Figure S27: Comparing split-terminator switch performance for terminator duplex length |d| = 40 nt, 30 nt, 20 nt, and 10 nt in HEK 293T cells. (a) Split-terminator switch cgRNA and trigger with domain |d|$\in$ {10, 20, 30, 40} nt. See Table S11 for sequences; shorter terminator duplexes with |d| = 30 nt, 20 nt, and 10 nt are truncations of the design with |d| = 40 nt. (b) Expression of RNA trigger X (xrRNA + {10, 20, 30, or 40} nt + terminator hairpin) toggles the cgRNA from OFF$\rightarrow$ON, leading to an increase in fluorescence. Transfection of plasmids expressing inducing dCas9-VPR, Phi-YFP target gene Y, and either: cgRNA + no-trigger control (OFF state), cgRNA + RNA trigger X (ON state). For this experiment only, flow cytometry was performed with an Accuri C6 flow cytometer. For each set of conditions, 50,000 cells were collected from a single replicate well, which was gated for live cells, single cells, and highly-transfected cells (as illustrated in Figure S7) except that transfection was gated based only on the cgRNA plasmid transfection control (miRFP670+), yielding approximately 2% of the cells. Bar graph depicts mean single-cell fluorescence over approximately 1000 cells for $N = 1$ replicate well.

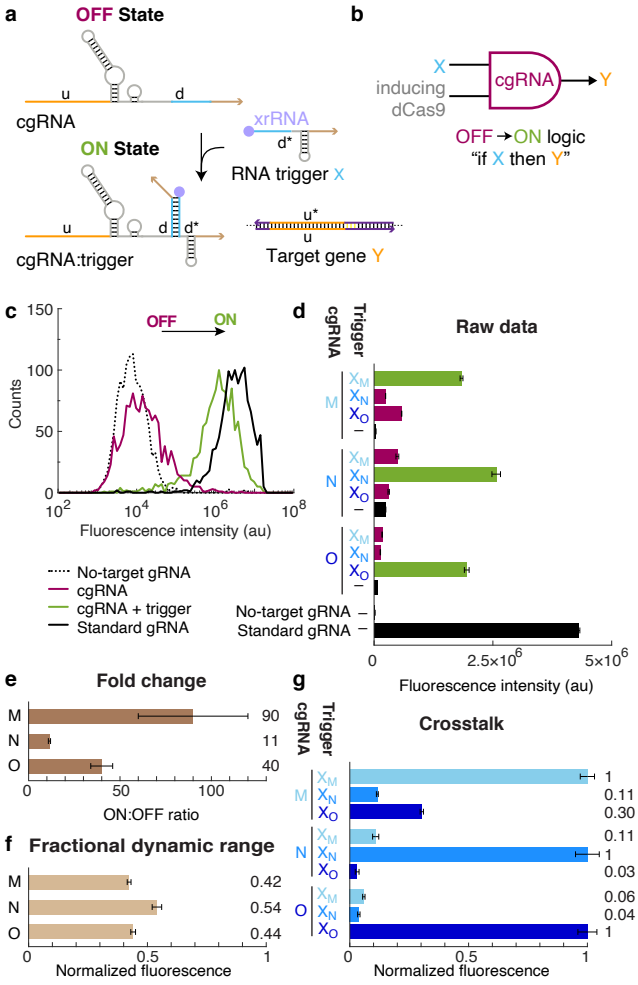

Figure S28: Full characterization of allosteric OFF→ON split-terminator switch performance with |d| = 10 nt and a 5′ xrRNA on the trigger in HEK 293T cells (cf. Figure 5 with |d| = 4 nt and no xrRNA on the trigger). (a) cgRNA mechanism: the constitutively inactive cgRNA is activated by hybridization of RNA trigger X. Designed 10 bp terminator duplex (cgRNA domain "d" and trigger domain "d*"). See Table S12 for sequences. (b) Conditional logic: "if X then Y". (c) Expression of RNA trigger X (xrRNA + 10 nt + terminator hairpin) toggles the cgRNA from OFF→ON, leading to an increase in fluorescence. Single-cell fluorescence intensities via flow cytometry. Transfection of plasmids expressing inducing dCas9-VPR, Phi-YFP target gene Y, and either: no-target gRNA that lacks target-binding region + no-trigger control (ideal OFF state), cgRNA + no-trigger control (OFF state), cgRNA + RNA trigger X (ON state), standard gRNA + no-trigger control (ideal ON state). Programmable conditional regulation using 3 orthogonal cgRNAs (M,N,O). (d) Raw fluorescence depicting OFF→ON conditional response to cognate trigger. (e) Fold change = ON/OFF. (f) Fractional dynamic range = (ON − OFF)/(ideal ON − ideal OFF). (g) Crosstalk = (SIG$_p$ − OFF)/(ON − OFF) where SIG$_p$ corresponds to signal for cgRNA + trigger p for $p \in \{\mathrm{X_M}, \mathrm{X_N}, \mathrm{X_O}\}$. Bar graphs depict mean ± estimated standard error of the mean (with uncertainty propagation) calculated based on the mean single-cell fluorescence over 1244–2313 cells for each of $N = 3$ replicate wells.

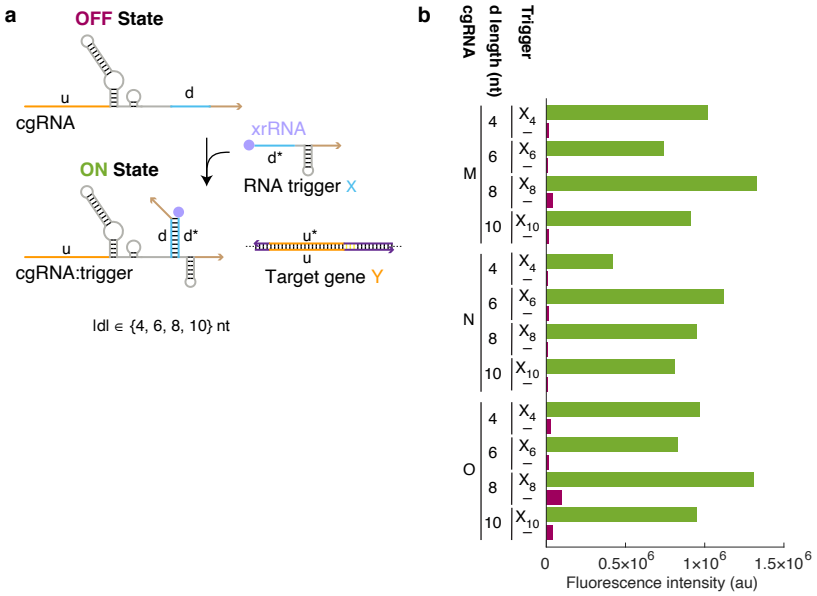

Figure S29: Comparing split-terminator switch performance for terminator duplex length |d| = 10 nt, 8 nt, 6 nt, and 4 nt in HEK 293T cells. (a) Split-terminator switch cgRNA and trigger with domain |d|$\in$ {4, 6, 8, or 10} nt. See Table S12 for sequences; shorter terminator duplexes with |d| = 8 nt, 6 nt, and 4 nt are truncations of the design with |d| = 10 nt. (b) Expression of RNA trigger X (xrRNA + {4, 6, 8, or 10} nt + terminator hairpin) toggles the cgRNA from OFF$\rightarrow$ON, leading to an increase in fluorescence. Transfection of plasmids expressing inducing dCas9-VPR, Phi-YFP target gene Y, and either: cgRNA + no-trigger control (OFF state), cgRNA + RNA trigger X (ON state). Bar graph depicts mean single-cell fluorescence over 1864–4155 cells for $N = 1$ replicate well.

S6.7 Comparison of split-terminator switch performance using a trigger with and without a 5′-end Dengue xrRNA

Based on our experiences with the ON→OFF terminator switch, where appending an xrRNA to the 5′ end of the trigger dramatically improved performance (see Section S6.2), we performed all of the domain dimensioning studies for the OFF→ON split-terminator switch using triggers with an xrRNA appended to the 5′ end (see Section S6.6). Here, we checked the performance of split-terminator switch cgRNAs (|d| = 4 nt) using triggers with and without a 5′ Dengue xrRNA. For the split-terminator switch, we found that adding the Dengue xrRNA to the 5′ end of the trigger was slightly detrimental to performance (Figure S30). Without the xrRNA, the ON state is slightly stronger and the OFF state is slightly cleaner, leading to an increase in fold change due to the smaller denominator. This difference in the efficacy of xrRNA triggers for the two cgRNA mechanisms may derive from the fact that for ON→OFF logic (terminator switch), the trigger is expected to function in the absence of dCas9 (Figure S14), while for OFF→ON logic (split-terminator switch), the trigger is expected to function in complex with dCas9 (Figure S15), potentially leading to differential degrees of protection from the protein effector.

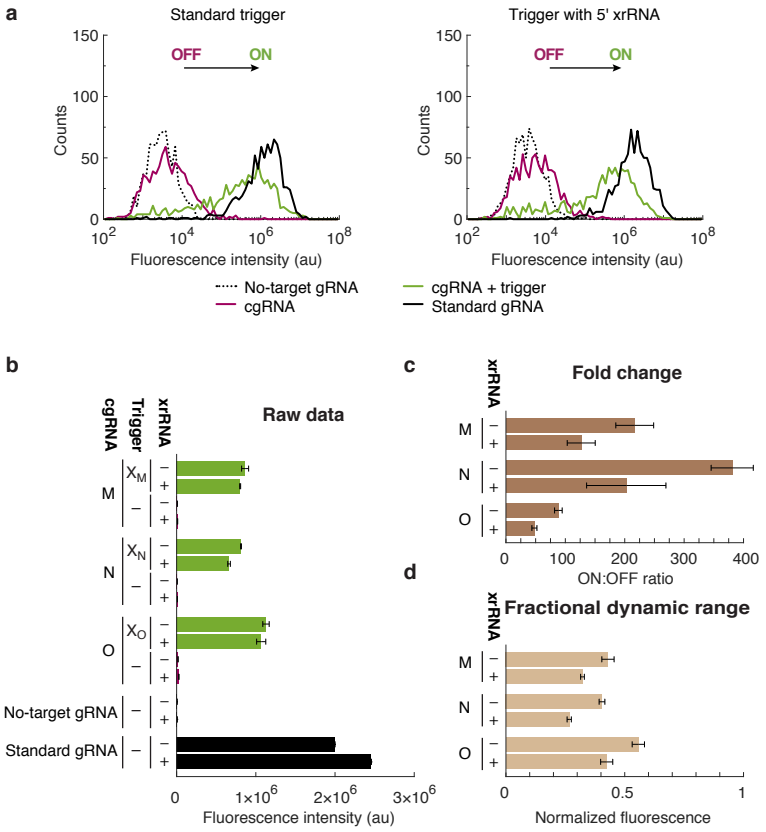

Figure S30: Comparison of split-terminator switch performance using triggers with and without a 5′ Dengue xrRNA in HEK 293T cells. Expression of RNA trigger X (±xrRNA + 4 nt + terminator hairpin) toggles the cgRNA from OFF→ON, leading to an increase in fluorescence. Transfection of plasmids expressing inducing dCas9-VPR, Phi-YFP target gene Y, and either: no-target gRNA that lacks target-binding region + no-trigger control (ideal OFF state), cgRNA + no-trigger control (OFF state), cgRNA + RNA trigger X (ON state), standard gRNA + no-trigger control (ideal ON state). The no-trigger control uses a random pool of triggers to provide a sequence-generic approximation of the metabolic load of trigger expression. Programmable conditional regulation using 3 orthogonal cgRNAs (M, N, O). Sequences are provided in Tables S4 and S6. (a) Single-cell fluorescence intensities for cgRNA M (replicate 1) using a standard trigger (left) or a trigger with a 5′ Dengue xrRNA (right). (b) Raw fluorescence depicting OFF→ON conditional response to cognate trigger. (c) Fold change = ON/OFF. (d) Fractional dynamic range = (ON − OFF)/(ideal ON − ideal OFF). Bar graphs depict mean ± estimated standard error of the mean (with uncertainty propagation) calculated based on the mean single-cell fluorescence over 1537–5081 cells for each of $N = 3$ replicate wells.

References

(1) Kieft, J. S., Rabe, J. L., and Chapman, E. G. (2015) New hypotheses derived from the structure of a flaviviral Xrn1-resistant RNA: Conservation, folding, and host adaptation. *RNA Biology* 12, 1169–1177.

(2) Boehm, V., Gerbracht, J. V., Marx, M.-C., and Gehring, N. H. (2016) Interrogating the degradation pathways of unstable mRNAs with XRN1-resistant sequences. *Nat. Commun.* 7, 13691.

(3) Zadeh, J. N., Steenberg, C. D., Bois, J. S., Wolfe, B. R., Pierce, M. B., Khan, A. R., Dirks, R. M., and Pierce, N. A. (2011) NUPACK: Analysis and design of nucleic acid systems. *J. Comput. Chem.* 32, 170–173.

(4) Wolfe, B. R., Porubsky, N. J., Zadeh, J. N., Dirks, R. M., and Pierce, N. A. (2017) Constrained multistate sequence design for nucleic acid reaction pathway engineering. *J. Am. Chem. Soc.* 139, 3134–3144.

(5) Zadeh, J. N., Wolfe, B. R., and Pierce, N. A. (2011) Nucleic acid sequence design via efficient ensemble defect optimization. *J. Comput. Chem.* 32, 439–452.

(6) Wolfe, B. R., and Pierce, N. A. (2015) Sequence design for a test tube of interacting nucleic acid strands. *ACS Synth. Biol.* 4, 1086–1100.

(7) Serra, M. J., and Turner, D. H. (1995) Predicting thermodynamic properties of RNA. *Methods Enzymol.* 259, 242–261.

(8) Hanewich-Hollatz, M. H., Chen, Z., Hochrein, L. M., Huang, J., and Pierce, N. A. (2019) Conditional guide RNAs: Programmable conditional regulation of CRISPR/Cas function in bacterial and mammalian cells via dynamic RNA nanotechnology. *ACS Cent. Sci.* 5, 1241–1249.

(9) Chen, B., Gilbert, L. A., Cimini, B. A., Schnitzbauer, J., Zhang, W., Li, G. W., Park, J., Blackburn, E. H., Weissman, J. S., Qi, L. S., and Huang, B. (2013) Dynamic imaging of genomic loci in living human cells by an optimized CRISPR/Cas system. *Cell* 155, 1479–91.

(10) Farzadfard, F., Perli, S. D., and Lu, T. K. (2013) Tunable and multifunctional eukaryotic transcription factors based on CRISPR/Cas. *ACS Synth. Biol.* 2, 604–613.

(11) Shcherbakova, D. M., Baloban, M., Emelyanov, A. V., Brenowitz, M., Guo, P., and Verkhusha, V. V. (2016) Bright monomeric near-infrared fluorescent proteins as tags and biosensors for multiscale imaging. *Nat. Commun.* 7, 12405.

(12) Mali, P., Aach, J., Stranges, P. B., Esvelt, K. M., Moosburner, M., Kosuri, S., Yang, L., and Church, G. M. (2013) CAS9 transcriptional activators for target specificity screening and paired nickases for cooperative genome engineering. *Nat. Biotechnol.* 31, 833–838.

(13) Nissim, L., Perli, S. D., Fridkin, A., Perez-Pinera, P., and Lu, T. K. (2014) Multiplexed and programmable regulation of gene networks with an integrated RNA and CRISPR/Cas toolkit in human cells. *Mol. Cell* 54, 698–710.

(14) Ferry, Q. R. V., Lyutova, R., and Fulga, T. A. (2017) Rational design of inducible CRISPR guide RNAs for de novo assembly of transcriptional programs. *Nat. Commun.* 8, 2109.

(15) Chavez, A., Scheiman, J., Vora, S., Pruitt, B. W., Tuttle, M., Iyer, E. P. R., Lin, S., Kiani, S., Guzman, C. D., Wiegand, D. J., Ter-Ovanesyan, D., Braff, J. L., Davidsohn, N., Housden, B. E., Perrimon, N., Weiss, R., Aach, J., Collins, J. J., and Church, G. M. (2015) Highly efficient Cas9-mediated transcriptional programming. *Nat. Methods* 12, 326–328.

(16) Gao, Z., Herrera-Carrillo, E., and Berkhout, B. (2018) Delineation of the exact transcription termination signal for type 3 polymerase III. *Mol. Ther. Nucleic Acids* 10, 36–44.

(17) Wang, D., Zhang, C., Wang, B., Li, B., Wang, Q., Liu, D., Wang, H., Zhou, Y., Shi, L., Lan, F., and Wang, Y. (2019) Optimized CRISPR guide RNA design for two high-fidelity Cas9 variants by deep learning. *Nat. Commun.* 10, 4284.

(18) Pijlman, G. P., Funk, A., Kondratieva, N., Leung, J., Torres, S., van der Aa, L., Liu, W. J., Palmenberg, A. C., Shi, P.-Y., Hall, R. A., and Khromykh, A. A. (2008) A highly structured, nuclease-resistant, noncoding RNA produced by flaviviruses is required for pathogenicity. *Cell Host Microbe* 4, 579–591.

(19) Chapman, E. G., Costantino, D. A., Rabe, J. L., Moon, S. L., Wilusz, J., Nix, J. C., and Kieft, J. S. (2014) The structural basis of pathogenic subgenomic flavivirus RNA (sfRNA) production. *Science* 344, 307–310.

(20) MacFadden, A., O'Donoghue, Z., Silva, P. A. G. C., Chapman, E. G., Olsthoorn, R. C., Sterken, M. G., Pijlman, G. P., Bredenbeek, P. J., and Kieft, J. S. (2018) Mechanism and structural diversity of exoribonuclease-resistant RNA structures in flaviviral RNAs. *Nat. Commun.* 9, 119.